Thesis for The Degree of Licentiate of Philosophy

Producing Dark Matter at Particle Accelerators

Extending the landscape and performing global fits of Light Dark Matter theories

Taylor Rose Gray

Department of Physics
Chalmers University of Technology
Gothenburg, Sweden, 2024

Producing Dark Matter at Particle Accelerators
Extending the landscape and performing global fits of Light Dark Matter theories

Taylor Rose Gray

Department of Physics
Division of Subatomic, High Energy, and Plasma Physics
Chalmers University of Technology
SE-412 96 Gothenburg,
Sweden
Phone: +46(0)31 772 1000

Printed by Chalmers Digitaltryck,
Gothenburg, Sweden 2024.

Producing Dark Matter at Particle Accelerators

Extending the landscape and performing global fits of Light Dark Matter theories

Taylor Rose Gray

Department of Physics
Chalmers University of Technology

Abstract

There is overwhelming evidence for the existence of an unknown and dark mass in the universe from several different observations. This missing mass has been coined dark matter (DM), with one hypothesis being that its nature is a new type of particle which interacts minimally with ordinary matter. Major experimental efforts attempting to search for interactions between DM and ordinary matter are currently in place, with no convincing evidence of discovery so far. These experiments have largely been geared for DM with masses O(GeV-TeV), with the main search channel being nuclear recoils from DM scattering. However, DM with lighter masses, O(MeV-GeV), have been gaining significant interest recently since they can account for the measured cosmological DM relic abundance while evading nuclear recoil direct detection constraints. Since such light DM does not carry enough momentum to be probed optimally via nuclear recoils, other search strategies such as direct detection via electron recoils and accelerators are ideal for this mass range.

Here we study the vast theory potential of accelerator based experiments, in particular fixed target experiments, on motivated sub-GeV DM models. In Paper I, we consider two theoretical frameworks for spin-1 sub-GeV DM, so called simplified and SIMP models, both of which are testable by current and future experiments such as the upcoming (Light Dark Matter eXperiment) LDMX. We find that simplified models are subject to strong bounds from experiments, cosmological observations, and unitarity. However SIMPs, a more sophisticated framework for spin-1 DM, are not subject to unitarity violations and current experimental constraints, while being consistent with the relic abundance measurement and in reach of near future experimental sensitivities.

There is a growing number of constraints from laboratory experiments and astrophysical and cosmological observations on sub-GeV DM, each giving information on the viable parameter space not yet excluded. In Paper II, we compare these observations with the predictions of two sub-GeV DM models (Dirac fermion and complex scalar DM). We perform this comparison within frequentist and Bayesian global analyses using the Global And Modular BSM Inference Tool (GAMBIT) extended in this work. We infer the regions of parameter space preferred by current data, and compare with projections of near future experiments.

List of Publications

Appended publications

This thesis is based on the following publications (note alphabetical author name ordering in HEP):

[**Paper I**] R. Catena, T. R. Gray, *Spin-1 Thermal Targets for Dark Matter Searches at Beam Dump and Fixed Target Experiments* *JCAP vol. 11, p. 058 2023. DOI: 10.1088/1475-7516/2023/11/058. arXiv: 2307.02207 [hep-ph]* .

[**Paper II**] S. Balan, C. Balázs, T. Bringmann, C. Cappiello, R. Catena, T. Emken, T. Gonzalo, T. R. Gray, W. Handley, Q. Huynh, F. Kalhoefer, A. Vincent, *Resonant or asymmetric: The status of sub-GeV dark matter arxiv: 2405.17548 [hep-ph].* [Submitted to JCAP]

Other publications

[**a**] C. Cosme, M. Dutra, S. Godfrey, T. R. Gray, *Testing freeze-in with axial and vector Z' bosons* *JHEP vol. 09 p. 056 2021. DOI: 10.1007/JHEP09(2021)056. arXiv: 2307.02207 [hep-ph]* .

Statement of Contributions

- **Paper I:** My contributions of this paper included calculations of the relic density (which used my code), annihilation cross sections, and helicity amplitudes for unitarity considerations. I extended the MC software for simulations of DM production at beam dump experiments to include additional particle physics models, and performed these simulations for our models. I included all other relevant experiments in the analysis to generate the figures. I also contributed to interpretation of the results along with my supervisor, Riccardo Catena.
- **Paper II:** As one of the three corresponding authors in this paper, my main responsibility was the fixed target experiment likelihoods. This involved extending the MC simulation software to include our models, running simulations of relevant experiments for each model, tabulating the results, and implementing this data into the Collderbit GAMBIT module along with code for reading and interpolating the data in addition to the likelihood calculation.

Acknowledgments

This reseach is funded by the Knut and Alice Wallenberg project grant Light Dark Matter (Dnr. KAW 2019.0080).

I first would like to thank my PhD supervisor Riccardo Catena for all that he has and continues to teach me along with his consistent support. I am truly so grateful to be a part of his research group and I look forward to the rest of my PhD under his supervision. Thank you to past and present members of our group and division at Chalmers, to my collaborators in the sub-GeV GAMBIT project, and to those at Lund University on LDMX for their invaluable input during our weekly group meetings. To my colleagues/friends at the department, thank you for providing fruitful discussions during coffee regarding interesting physics such as the implications from the variation of the Planck constant.

Contents

Part I

Chapter 1

Introduction

Dark matter (DM), which we know to exist from its influence on cosmological and astrophysical observations, and which is fundamental to the galactic structure of the universe we live in, has an unknown nature. So far, there is lack of any convincing discovery signal of a particle that could explain the gravitational evidence we observe. This problem, which follows from years of scientific advancement in the fields of astronomy, cosmology, classical mechanics, quantum mechanics, and more is one of the greatest of our time. Let us take a step back in time to the 1500s, prior to the current understanding of the universe that we have today to put this problem into context.

It took more than 100 years for Copernicus' initially controversial heliocentric model of the solar system to become accepted in the scientific community. Prior to 1543 when Copernicus' *On the Revolutions of the Heavenly Spheres* [1] was published, the earth was thought to be the center of the universe. Later, using Tycho Brahe's measurements, Johannes Kepler formulated the laws of planetary motion. Galileo used a telescope for the first time to observe planets and stars, finding the moons of Jupiter thus proving Copernicus' hypothesis of a non-geocentric solar system. He also made vital contributions to the understanding of the laws of motion, which was important for Isaac Newton to formulate the laws of gravitation. In 1687, the phenomenon of gravitational attraction experienced between astronomical bodies was connected with the tendency for objects here on earth to fall to the floor, through Newton's law of gravitation [2]. This fundamentally connects the seemingly separate worlds of astronomical bodies in outer space and our experienced lives on earth. Newton also discovered that light was made of several different colours, laying the grounds for spectroscopy, the foundation of observational astronomy [3].

All while, and long before, this important progress in our understanding of physics and astronomy was being made, astronomy was being used as a means of navigation and time keeping. Navigating the seas became easier using accurate measurements of the positions of stars from understanding planetary motion. Uncovering the laws of nature governing the universe has not only been to feed our curiosity, but also for practical applications leading to invaluable improvements in society.

After the discovery of Uranus in 1781, it was noticed that its orbit around the solar system's barycenter was slightly different than predicted by Newtonian gravity. One viable explanation for these perturbations in the orbit was that there exists a new planet beyond it. In 1846, Neptune was discovered after predicting its position using these perturbations from the expected orbit. This serves as an example how astronomical objects can be inferred from their gravitational influence on known and measurable objects. When deviations from the predicted motion of objects under gravity is discovered, it can be explained by one of two scenarios: 1. there is an undiscovered object which is influencing other objects gravitationally or 2. the current theory of gravity is incomplete.

Newtonian gravity works well for explaining objects falling on earth or many planetary orbits, although it was discovered that it fails to describe the observed precession of Mercury's perihelion. It was hypothesized at the time that there could exist another planet between the sun and Mercury, namely Vulcan, although no new planet was every observed and instead a new theory of gravitation was born. Einstein published his theories of special and general relativity [4], [5] in 1905 and 1915, respectively, where special relativity postulates that the speed of light is the same in all reference frames, and general relativity elegantly describes space and time as one entity. Newtonian gravity can only handle cases where gravitational fields are small and velocities are non-relativistic, outside of these realms general relativity is needed. For example, it is required for explaining phenomena such as Mercury's orbit (where the gravitational field from the sun is large) and for the accuracy of Global Positioning Systems (GPSs). There is even yet another proposed extension of the current framework of gravitation, namely Modified Newtonian Dynamics (MOND) [6], which attempts to provide an explanation for anomalous stellar and galactic dynamics. However, it is debated whether or not MOND is substantial, and whether a new unknown massive object exists within galaxies instead. Later we will discuss the existence of this unknown mass in much more detail.

Following the formulation of special and general relativity, Einstein's work [7] from recently after where a static closed model for the universe, was derived – setting the foundation for modern cosmology. Einstein introduced an additional term to his field equations, the cosmological constant, where this term counteracts the inward pull of gravity in the universe. In 1929, Edwin Hubble measured the velocities of galaxies and discovered that they are receding away from us [8], thus the universe is expanding. Einstein then assumed that the cosmological constant term is no longer needed. Even prior to these observations of the expanding universe, Georges Lemaître worked on an expanding universe solution to Einstein's equations, independently of Alexander Friedmann. Lemaître had the idea that the universe began from one point and then expanded radially, being now known as the Big Bang theory [9], [10]. Later on, in 1998, the acceleration of the expansion of the universe was measured using distant supernovae independently by two groups, and it was concluded that the expansion of the universe is speeding up [11], [12]. With this discovery, Einstein's cosmological constant regained validity as it represents

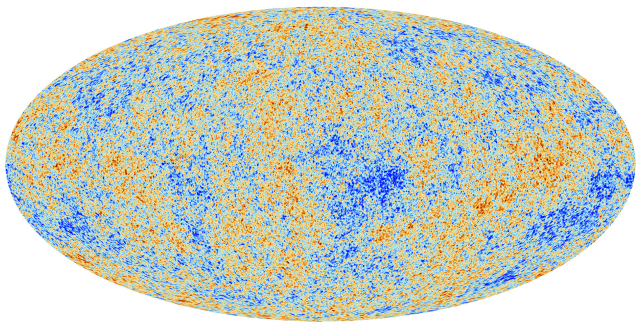

Figure 1.1: Sky map of the CMB photons observed by Planck [13]. Colours show the temperature of these photons, with red being slightly hotter and blue slightly colder. The average temperature is 2.7 Kelvin, and the difference between the blue and the red is on the order of 10^{-5} Kelvin.

this unknown repulsive force now called dark energy.

If the universe began from a single point, the universe would have been very dense and hot in its earliest times. Its temperature would have been so high, approximately 10^{32} Kelvin after 1 second, that atoms could not even form yet. In this dense cosmic soup of free electrons and nuclei, photons could not travel far without interacting, similar to fog. After 380 thousand years, when the universe expanded and cooled to ~ 3000 Kelvin, electrons combined with hydrogen and helium nuclei and photons could now travel freely, thus the universe became transparent. These first photons, from when the universe first became transparent, are the Cosmic Microwave Background (CMB), our earliest probe of the universe using light measurements. The CMB was first predicted by George Gamow, Ralph Alpher, and Robert Herman in 1948 [14]–[16], and was first measured in 1965 unintentionally as excess noise in a radio receiver [17], [18]. Fig. 1.1 is a skymap of the CMB temperature measured by the Planck satellite [13]. The anisotropies of the CMB embed information on the abundances of baryons and other content (which will be discussed in the following sections) in the universe.

The *ultraviolet catastrophe* was realized at the end of the 19^{th} century, when experimental results of blackbody radiation (spectra of intensity as a function of wavelength of emitted light of almost perfect absorbers) did not agree with theoretical predictions. At the time, theory predicted that the energy emitted at smaller wavelengths grew to infinite – something clearly unphysical. In 1900, Max Planck solved this problem by introducing *quanta*, discrete energy levels that the atoms in a blackbody can have. These discrete energy levels are integer multiples of a base energy unit proportional to Planck's constant, h. At the time, the deeper consequences of these discretized energies were not yet realized; it was viewed merely as a mathematical trick to fit observations. Einstein also used Planck's quanta to explain the *photoelectric effect*, where light incident on a metal ejects electrons. A wave description of light was not consistent with the observations of the photoelectric effect, although other phenomena such as

those in thermodynamics required both a wave and a quantized description of light – two inconsistent frameworks.

In 1913, Niels Bohr studied the Rutherford nuclear model, one of the models of the atom at the time. In the Rutherford picture, heavy positively charged nuclei are orbited by much lighter negatively charged electrons, similarly to a mini solar system. There were a couple of problems with this picture. For one, the emission and absorption spectra of hydrogen consisting of discrete lines could not be explained. In addition, this atom could not be stable, as the negative charge, attracted to the positively charged nucleus, would in fact spiral in towards the nucleus. In order to fix this description of the atom, Bohr proposed a new model. In this model, the electron orbits the nucleus in discrete orbits – quantized angular momentum, and when the electron is jumping between these orbits, light is emitted or absorbed at a specific energy. Here, Planck's quantum theory was being applied to the model of the atom. Despite the inevitable realization that this light of specific energy being absorbed or emitted in the atom is indeed the same *light quanta* that Einstein introduced, Bohr was rather reluctant to accept them as the same. Later, Einstein was able to connect the Bohr atom to blackbody radiation. He linked blackbody radiation to discrete energy levels and stated that the transitions could only be predicted in a probabilistic way. Although, there were missing pieces to Bohr's atomic theory; atoms with more than one electron (every element but hydrogen) could not be predicted well with this theory.

In 1925, Werner Heisenberg developed a mathematical formalism for quantum mechanics [19], based on matrix mechanics. At the same time, Erwin Schrödinger presented his formalism involving matter waves represented as wavefunctions [20]. Many technologies rely on the developments of quantum mechanics, such as magnetic resonance imaging used in medicine, lasers, solar cells, atomic clocks, and quantum computing.

The development of special relativity and quantum mechanics made way for their combination, quantum field theory, the theoretical framework used in describing the physics of the smallest known constituents of matter. We rely on the methods of quantum field theory in this thesis to model and characterise these constituents of matter and the forces that act on them, similarly for DM. Specifically, this work hypothesizes viable theoretical scenarios for the nature of DM, describing its fundamental properties and interactions with other species using quantum field theory, and computes the expected signals and sensitivity at experiments searching for DM.

This thesis is organized as follows: First Chapter 1 provides an introduction to the Standard Model of particle physics and its shortcomings, introducing a particular shortcoming which is the topic of this thesis, DM. The evidence for the existence of DM is discussed in this chapter as well. Chapter 2 discusses the candidates and early universe production of particle DM provides an outline of the various DM search efforts, followed by motivation for the search for sub-GeV mass DM. Various accelerator bases experiments searching for DM production, in particular fixed target experiments are explained in Chapter 3. Theoretical models of spin-1 sub-GeV DM, based on Paper I, are considered in Chapter 4, while global fits of sub-GeV DM from Paper II in Chapter 5.

Finally, future and ongoing work along with a summary of this thesis is given in Chapter 6.

1.1 The Standard Model

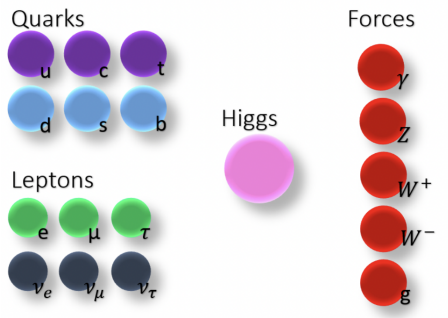

Figure 1.2: The particles that make up the SM of particle physics.

The particles which make up the Standard Model (SM) of particle physics, the current best theory describing the constituents of matter and their interactions, are shown in Fig. 1.2. These particles, grouped into quarks, leptons, force carrier bosons, and the Higgs, are involved in electroweak theory describing electromagnetism and the weak interaction, and quantum chromodynamics (QCD) describing the strong interaction.

The SM has been highly successful theory, describing a number of phenomena. For instance, the Higgs boson was first predicted in 1964, and then in 2012 it was discovered experimentally by the ATLAS and the CMS collaborations [21], [22]. Other particles such as the top quark [23], and the W and Z bosons [24] were discovered after being predicted by the SM. As another incredible example of the SM's success, the electron magnetic dipole moment measurement agrees with SM theory predictions to one part in 10^{12} [25].

Although the SM works well in predicting many observations, the SM is not (yet) a complete theory, lacking the ability to explain many phenomena. These shortcomings have opened up a new field of particle physics, beyond the SM (BSM) physics, where these missing pieces are addressed with new physics. The following is a non-exhaustive list of some of the most studied phenomena lacking in the SM:

Gravity: As of yet, there is no known way to unify our current best theory of gravitation, namely general relativity, with the other three forces (electromagnetic, weak, and strong) explained by the SM, since general relativity breaks down in the quantum realm. In addition, there has not been a force carrier particle discovered for gravity, namely a graviton [26]. There are ongoing efforts to develop a *theory of everything*, such as string theory [27], which would include the unification of gravity and the SM.

Dark Energy: As mentioned above, dark energy, or the origin of cosmic accelerated expansion, is unknown and unexplained by the SM [28]. One explanation is that dark energy is a cosmological vacuum energy, although this leads to results for the theoretically calculated energy of this quantum vacuum far too large [29]. Another possibility is that dark energy comes from new physics, such as from a light scalar field [30]–[34].
Baryon Asymmetry: The mechanism explaining the asymmetry in the amount of matter to anti-matter, baryogenesis, is an open question [35], [36]. There must exist an asymmetry in the amount of matter compared to anti-matter, since if they both existed in equal amounts, all matter would have annihilated away in the early universe. Interestingly, you and I both exist as beings made of matter, gravitationally bound to a planet made of matter, within a galaxy of matter, etc.
Hierarchy Problem: The hierarchy problem refers to the large difference between the Higgs and gauge boson masses compared to the Planck mass (the scale of gravity). Supersymmetry has been one well studied option for accounting for this problem.
Neutrino Masses: The SM does not predict that neutrinos have any mass, which is in conflict with measurements of neutrino oscillations indicating that they do indeed have mass [37]–[39].
Dark Matter: Finally we have DM, the topic of this thesis. DM is the term used to call the elusive form of matter which interacts minimally via electromagnetism, that we have evidence of through gravitational implications in astrophysics and cosmology, as we discuss in the following section. DM cannot be accounted for by the SM, so there must exist new physics to explain it. The following sections will focus on the following questions: How do we know about the existence of DM? What are some ways it could have been produced in the early universe? What could be its particle nature? What are the ways in which we are trying to detect it?

1.2 The Unknown Mass

It is not trivial to pin point the first discussions and scientific work considering the existence of unobserved (or dark) astronomical objects [40]. For example, in 1844 Friederich Bessel realized that there must exist unobserved stars influencing the motion of stars Sirius and Procyon [41] - similarly to the discovery of the planet Neptune, this marks a significant occasion in history where an astronomical object was anticipated solely based on its gravitational interactions.

It turns out that the amount of mass observed in galaxies is not consistent with theoretical predictions. In 1904, Lord Kelvin noticed that the mass in our galaxy, the Milky Way, estimated from measurements of velocities of stars, must include dark bodies which we cannot see [42].

Often you will hear this story begin in 1933 with the astronomer Fritz Zwicky and his comparison between measured versus theoretically predicted velocities of galaxies within the Coma Cluster. [43]. Using the virial theorem,

Figure 1.3: [44]

Zwicky calculated what the velocities of 800 galaxies each $\sim 10^9$ solar masses within a radius of one million light years should be theoretically and found a value of approximately 80 km/s. However, he found that the measurements of velocities using redshifts are approximately 1000 km/s. This over an order of magnitude discrepancy called for the existence of some unknown missing matter, dubbed *dark matter*.

The Bullet Cluster (also known as 1E 0657-56), shown in Fig. 1.3, magnificently demonstrates the existence of DM and the necessity for it to be a new type of matter distinct from ordinary matter. This false colour image is of the collision of two galaxy clusters, where each cluster has an ordinary matter component and a DM component. The white and yellow spots are other galaxies in the distance, taken in the optical by the Magellan and the Hubble Space telescopes. The red is the X-rays detected by the Chandra telescope, which shows where the baryonic/ordinary matter (hydrogen gas) exists within the clusters. Finally, the blue is where most of the mass is concentrated from gravitational lensing[1] measurements. As evident in Fig. 1.3, there is a mismatch between the red and blue regions, namely the expected and the measured locations of the mass in the clusters. Notice also that the blue region has moved further from the collision center than the red regions, showing the slowing of the gas from frictional forces and the blue matter's lack of friction. With this, we have evidence that the majority of the mass in these galaxy clusters demonstrating this particular behaviour is some additional invisible matter, DM, which interacts very weakly. This is the most famous example, although there are several other examples of galaxy clusters demonstrating the existence of DM.

Zooming into individual galaxies; the shapes of the rotation curves of

[1] Gravitational lensing is the effect where gravity from a massive object causes light passing near it to bend. By measuring the distorted shapes of luminous objects under this effect by performing gravitational lensing surveys, the distribution of mass can be determined.

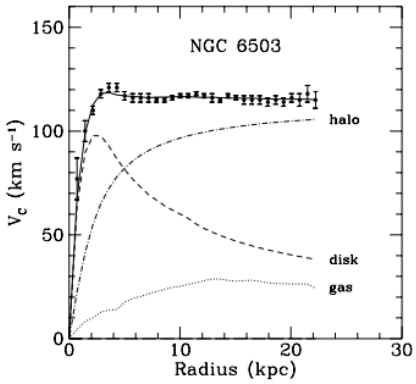

Figure 1.4: Rotational velocities of stars in the spiral galaxy NGC 6503 [45]. The points with error bars are measurements using red shifts. The dashed curve labeled "disk", the dotted curve labeled "gas", the dash dotted line labeled "halo", and the solid curve going through the data are theoretical curves considering only ordinary matter, gas, a DM halo, and ordinary matter with a DM halo added in quadrature, respectively.

galaxies also demonstrate the existence of DM [45], [46]. It is expected that after a sufficient distance from the center of the galaxy, the radial velocities, $v(r)$, will decrease with increasing radius, r, with the relationship,

$$v(r) = \sqrt{\frac{GM(r)}{r}}, \tag{1.1}$$

where G is the gravitational constant and $M(r) = 4\pi \int_0^r \rho(r')r'^2 dr'$, with $\rho(r)$ as the mass density distribution of the DM around the galaxy – the DM halo. This is in contradiction to measurements where the radial velocity curves instead flatten out [45], [46]. As an example, we take the rotation curve of spiral galaxy galaxy NGC 6503, as shown in Fig. 1.4. Here it is evident that only considering the ordinary matter component leads to predictions that do not match the data. There must be a DM halo component in order to reproduce the flattened rotation curves. The DM halos that are hypothesized to exist as the major component of galaxies are predicted to have a spherical shape[2] distributed according to rotation curve observations with a mass density following $\rho \sim r^{-2}$. However, the density profiles of DM in the center regions of galaxies differ whether considering simulations or observational data [48]. Hydrodynamical N-body simulations of galaxy formation lead to central profiles that are *cuspy* following $\rho \sim 1/r$ at small r [49], while the data is instead consistent with a constant density *core* where $\rho \sim r^0$ [50]. This disagreement is called the "core-cusp problem", which has had many proposed solutions [51].

During the 1970s, it became accepted that galaxies are enveloped inside of these massive DM halos [52], [53]. These halos provide the galaxies with

[2]It is plausible that the DM halo shapes are not exactly spherical [47].

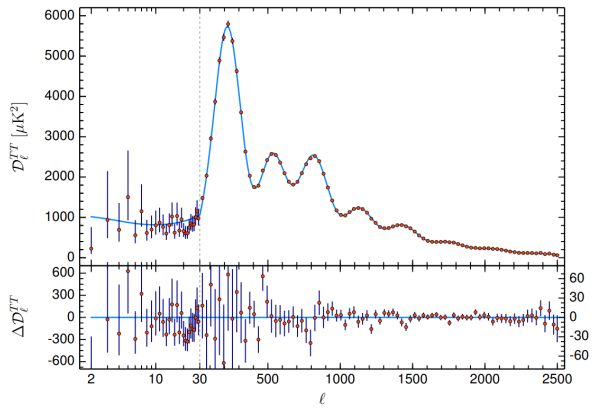

Figure 1.5: The temperature power spectrum of the CMB [13], where the temperature fluctuations are plotted versus multipole l. The measurements made by the Planck satellite are plotted in red along with their error bars, and the ΛCDM theoretical best fit is plotted in light blue.

large gravitational potential wells in which ordinary matter can cool and form into galaxies [54]. From simulations of structure formation, the universe as we know it today cannot exist without a significant DM component. Without DM present, galaxies start forming after recombination[3] – which is inconsistent with the galaxy we observe today. Density fluctuations of baryonic matter do not increase with time before matter-radiation decoupling due to the photon pressure from frequent Compton scattering. Therefore, DM is necessary to have the galactic structure in which we live.

The final piece of evidence for DM to mention; the CMB anisotropies. The oscillations of the photon and baryon plasma in the early universe cause the angular fluctuations of the CMB temperature. These oscillations are caused by the competing forces from gravity and photon pressure. In order to quantify the temperature anisotropies, we compute the power spectrum - the angular correlation function of the temperature differences expanded in spherical harmonics, as shown in Fig. 1.5. The angular scales of the CMB are depicted by the peaks and troughs, which change with the abundance of DM, ordinary matter, and dark energy showing their individual contributions [55]. The blue curve in Fig. 1.5 is the best fit of the ΛCDM (Cold DM) model, the current best cosmological model [56]. The cosmological parameters that are fit include the abundance of baryons and DM in the universe, Ω_B and Ω_{DM}[4], where $\Omega_i \equiv \rho_i/\rho_c$, and the critical density is given by,

$$\rho_c \equiv \frac{3H_0^2}{8\pi G} \approx 1.05 \times 10^{-5}\text{GeV}^2\text{cm}^{-3}. \tag{1.2}$$

[3]Recombination is the cosmological epoch where the universe is cooled sufficiently for electrons and protons to form hydrogen atoms.

[4]Often (and later in this thesis) cosmological abundances are expressed in units of Ωh^2, in which H_0 is factored out.

The universe's energy budget is 69% dark energy, 26% DM, and 5% ordinary matter [13].

With this undeniable evidence for DM, existing at many scales and times in the universe, we arrive at attempting to solve one of the greatest scientific mysteries of our time: the nature of the majority of matter in the universe is unknown.

Chapter 2

Particle Dark Matter

2.1 Its Nature and Cosmological Origin

What could make up this mysterious matter causing measurable gravitational effects in astrophysical and cosmological objects? An obvious explanation is that DM is made up of ordinary matter compact objects that are simply less luminous. These objects include planets, brown/red/white dwarfs, neutrons stars, and black holes: categorized as Massive Astrophysical Compact Halo Objects (MACHO) [57]. MACHOs have mostly been ruled out as a plausible DM candidate because of the lack of them found in microlensing surveys [58], [59] and measurements of the baryon density (such as from the CMB [13]), leaving a small mass window of primordial black holes as technically viable DM candidates [60], [61].

Another explanation is that it is in fact not matter at all, but instead evidence for the necessity for a more complete theory of gravity such as MOND [6], [62], [63] as introduced earlier. MOND is able to explain some of the shapes of rotation curves, however MOND has trouble when it comes to observations of galaxy clusters and the CMB [64], [65].

In order to explain the total amount of DM and all of its gravitational evidence, the idea that DM is made up of particles similar to ordinary matter, became popular. Only interacting through the weak and gravitational forces, SM neutrinos were hypothesized to be DM. One of the problems with neutrinos is that they were hot (relativistic) during structure formation of galaxies [66], which is inconsistent with simulations of structure formation showing the need for cold (non-relativistic) DM [67]. Another problem is that there is a lower bound on the mass of galactic halo leptons called the "Tremaine-Gunn bound" [68], since the density of fermions cannot exceed that of a degenerate Fermi gas. Since neutrinos are the only stable and electromagnetically neutral particle in the SM, this leaves us with the need for a new type of particle beyond the SM for DM. Despite the lack of information we have on the nature of this mysterious matter, this new hypothetical particle must fulfil some criteria: stable on cosmological scales, weak enough interactions with ordinary matter consistent with null results at experiments, early universe production mechanism giving

rise to the observed relic abundance (see Section 2.1.1), non-relativistic during structure formation, and small enough self interactions consistent with cluster observations.

The Weakly Interacting Massive Particle (WIMP) [69]–[73] has been one of the most popular classes of DM candidates[1], arising from BSM theories such as supersymmetry or from theories that attempt to solve the hierarchy problem. Interestingly for this candidate, the observed relic abundance by Planck [13] is obtained through freeze-out while having a cross section and mass near the weak scale - this realization (or coincidence) has been coined the "WIMP miracle". WIMPs are classified to have a mass in the $\sim O(GeV)$ to $\sim O(100\,TeV)$ range. If the WIMP interacts through the SM weak force, it is subject to the Lee-Weinberg bound which sets a lower bound on the mass due to avoiding over production of the DM density [74]. However, this lower bound can be circumvented by the addition of a new gauge mediator, allowing for masses below a GeV.

2.1.1 Thermal Production: Freeze-Out

The cosmological abundance of DM is known from measurements of the CMB [13], however the precise history of how this abundance came to be is unknown. If we consider that DM was once in thermal equilibrium with the SM bath, the DM history will follow that of the *freeze-out* mechanism [75], [76]. There are other possible mechanisms that can produce the observed abundance of DM such as *freeze-in* [77], where DM was never in thermal equilibrium with the SM bath, but here we focus on DM produced through freeze-out.

The assumption that DM was once in thermal equilibrium with the SM bath is not far fetched since most other species were once in thermal equilibrium, sharing a common temperature T. Fig. 2.1 plots the evolution of the DM density, or yield (described below) as a function of time. If DM was in thermal equilibrium with the SM bath, the DM abundance (coloured solid curves), follows the equilibrium curve (dashed curve) until chemical decoupling - when the Hubble rate exceeds the production and annihilation rate of DM. At a certain temperature, the average kinetic energy of the SM bath species will not be sufficient to efficiently annihilate to produce DM. The temperature at which Boltzmann suppression occurs is whichever happens first: either when the abundance of the initial species become small due to their own Boltzmann suppression, or if the DM is more massive than the initial species, when the temperature drops below the mass of the DM. This Boltzmann suppression is the point at which the equilibrium density falls off exponentially, from the exponential in the Maxwell-Boltzmann distribution that decreases rapidly as temperature decreases. The interaction strength, or coupling, between the DM and SM or other dark sector particles, governed by the DM model influences

[1]The definition of WIMP in the literature is not fully consistent - some consider them to interact via the $SU(2)_L$ gauge bosons in the SM (via the weak force), while others consider them to interact through new interactions via a new mediator. Here we take them to be of mass $O(GeV)$ to $\approx O(100TeV)$ and produced through the freeze-out production mechanism, interacting via SM or BSM forces.

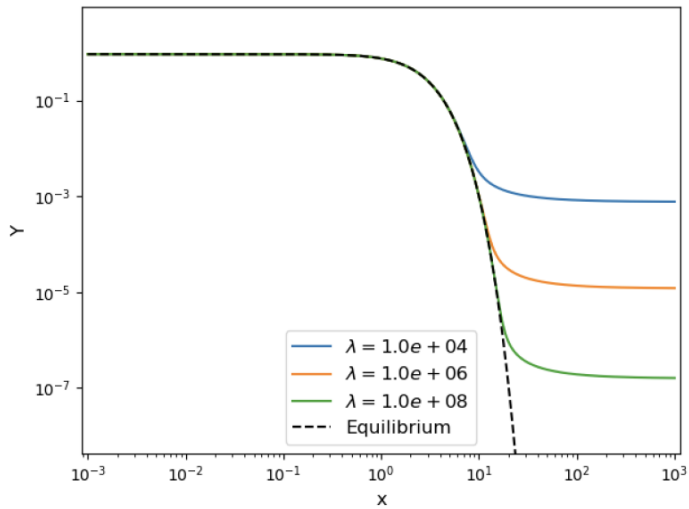

Figure 2.1: The evolution of the DM yield, or comoving number density, Y plotted vs $x \equiv m/T$ (a variable representing something similar to time) where m is a relevant mass scale and T is temperature. Coloured curves are the DM yield in the freeze-out scenario at various coupling strengths, and the dashed curve is the equilibrium yield assuming Maxwell-Boltzmann statistics.

how long the yield can follow the equilibrium curve until decoupling. Larger couplings lead to a smaller final DM yield.

The number density of a species of mass m and γ internal degrees of freedom in thermal equilibrium, assuming Maxwell Boltzmann statistics, follows [78],

$$n^{eq}(T) = \frac{\gamma m^2 T K_2\left(\frac{m}{T}\right)}{2\pi^2}. \tag{2.1}$$

Departures from thermal equilibrium were vital in establishing a relic - such as a DM relic and of course you, the reader. These departures from thermal equilibrium, namely the process of *decoupling* occurs when the interaction rate, Γ, of the given species with the other bath species drops below the Hubble expansion rate, H.

In order to calculate the abundance of DM for a given theoretical framework for DM, the decoupling must be treated by using the Boltzmann equation to compute the evolution of the particle's phase space distribution [75], [78]. You may refer to [75], [78], [79] for a review of equilibrium thermodynamics and more details on the Boltzmann equation. The number density n is governed by the Boltzmann fluid equation,

$$\dot{n} + 3Hn = R(t), \tag{2.2}$$

where R is the interaction rate density, the number of interactions per unit

time and volume,

$$R(t) = \frac{\gamma}{(2\pi)^3} \int C[f] \frac{d^3p}{E}, \tag{2.3}$$

where $C[f]$ is the collision operator[2] as a function of the distribution function f containing all particle number changing interactions, E is the energy, p is the momentum, and H is the Hubble rate. The Hubble rate describes the expansion rate of the universe,

$$H \equiv \frac{\dot{a}}{a} \tag{2.4}$$

where a is the scale factor. During the radiation dominated era the Hubble parameter is given by,

$$H(T) = \sqrt{\frac{8\pi^3}{90}} \frac{\sqrt{g_{*e}} T^2}{m_{Pl}}, \tag{2.5}$$

where $g_{*e}(T)$ is the effective number of degrees of freedom associated with energy [80] given by,

$$g_{*e} = \sum_{bosons\ i} \gamma_i \left(\frac{T_i}{T}\right)^4 + \frac{7}{8} \sum_{fermions\ j} \gamma_j \left(\frac{T_j}{T}\right)^4 \tag{2.6}$$

and m_{Pl} is the Planck mass.

Considering the process $i + j + \cdots \leftrightarrow k + l + \cdots$, if we are interested in the particle i,

$$\begin{aligned} R_i(t) &= \frac{\gamma_i}{(2\pi)^3} \int C[f] \frac{d^3p_i}{E_i} \\ &= \int d\Pi_i d\Pi_j \cdots d\Pi_k d\Pi_l \cdots (2\pi)^4 \delta^4(p_i + p_j + \cdots - p_k - p_l - \cdots) \\ &\quad \big[|\bar{M}|^2_{k+l+\cdots \to i+j+\ldots} f_k f_l \cdots (1 \pm f_i)(1 \pm f_j) \cdots \\ &\quad - |\bar{M}|_{i+j+\cdots \to k+l+\ldots} f_i f_j \cdots (1 \pm f_k)(1 \pm f_l) \cdots \big] \end{aligned} \tag{2.7}$$

where $|\bar{M}|^2$ is the squared amplitude averaged over initial and final spins[3], $d\Pi$ are the phase space differential elements,

$$d\Pi = \frac{\gamma d^3p}{(2\pi)^3 2E}, \tag{2.8}$$

and the $(1 \pm f)$ factors are the stimulated $(+)$ and blocking $(-)$ factors for final state bosons and fermions respectively.

Let us now define two useful parameters. To scale out the universe's expansion, we use the comoving number density or yield, Y, defined by,

$$Y \equiv \frac{n}{s}, \tag{2.9}$$

[2]The collision operator is defined as the rate of change of the distribution function of the species of interest due to collision processes such as scattering and annihilation.

[3]In cosmology we average over initial and final spins, rather than averaging over initial and summing over final spins, since we do not know the initial or final states.

where s is the entropy density. We use x as a parameter representing time in a convenient way,

$$x \equiv \frac{m}{T}, \tag{2.10}$$

where m is a relevant mass scale, usually set to be of the particle of interest, m_i.

Let us consider the process $34 \leftrightarrow 12$[4] where we are interested in calculating the final yield of particle 3, Y_∞. Let us also make a few assumptions that simplify the problem: assume charge-parity (time) invariance hence $|\bar{M}|^2_{12\to34} = |\bar{M}|^2_{34\to12}$, Maxwell Boltzmann statistics thus emitting the stimulated and blocking $(1 \pm f)$ factors, and that particle 3 is in thermal equilibrium until it decouples and moreover is in kinetic equilibrium during chemical decoupling. We write the Boltzmann eq, Equation 2.2, in terms of Y and x under these assumptions,

$$\frac{dY_3}{dx} = \sqrt{\frac{\pi}{45}} \frac{m_{Pl} m_3 g_*}{x^2} \langle \sigma v \rangle_{34\to12} \left((Y_3^{eq})^2 - Y_3^2 \right) \tag{2.11}$$

where Y^{eq} is the equilibrium yield given by,

$$Y_i^{eq} = \frac{n_i^{eq}}{s} = \frac{45 \gamma_i x^2 K_2(x)}{4\pi^4 g_{*s}}, \tag{2.12}$$

and the thermally averaged cross section is,

$$\langle \sigma v \rangle_{34\to12} = \frac{\int \sigma_{34\to12}(s_m - 4m_3^2)\sqrt{s_m} K_1\left(\frac{\sqrt{s_m}}{T}\right) ds_m}{8 m_3^4 T K_2\left(\frac{m_3}{T}\right)^2}. \tag{2.13}$$

Equation 2.11 is a differential equation with no analytic solution, therefore we must rely on numerical methods to solve it. However, in the case of freeze-out, if we can determine the freeze-out temperature T_F, the final present day yield can be approximated. After freeze-out, $Y^{eq} \ll Y$, so Y^{eq} in Equation 2.11 can be safely neglected.

We take the result of [75] (also see [79] for more details) for the yield of particle three at $t = \infty$, or the present day yield,

$$\frac{1}{Y_\infty} \approx \frac{1}{Y_f} + \int_0^{T_f} \sqrt{\frac{\pi}{45}} \frac{m_{Pl} m_3 g_*}{x^2} < \sigma v >_{34\to12} dT. \tag{2.14}$$

The freeze-out temperature can be calculated in two main ways. For the first method, we can numerically solve for T_f, or $x_f \equiv \frac{m_3}{T_f}$, using [75],

$$\left.\frac{dY_3^{eq}}{dx}\right|_{x_f} \approx -\sqrt{\frac{\pi}{45}} \frac{m_{Pl} m_3 g_*(x_f)}{x_f^2} \langle \sigma v \rangle_{34\to12}(Y_3^{eq}(x_f))^2 \left(\delta^2 + 2\delta\right) \tag{2.15}$$

where $\left.\frac{dY_3^{eq}}{dx}\right|_{x_f}$ is the derivative of $Y_3^{eq}(x)$ with respect to x evaluated at x_f, and we can take $\delta = 1.5$ [75]. The second method for calculating T_f is to take

[4] All other number changing processes such as $1 \to 2$ and $3 \to 2$ (where the latter is relevant for Paper I) must be considered when solving the Bolzmann equation.

the temperature at which the Hubble rate exceeds the annihilation rate of particle 3.

These methods of calculating the relic abundance of DM are used in both Paper I and II for determining the parameters consistent with the measured abundance, the so called *relic targets*.

2.2 Dark Matter Searches

In this section, we briefly outline the types of efforts that exist to search for signals from DM particles.

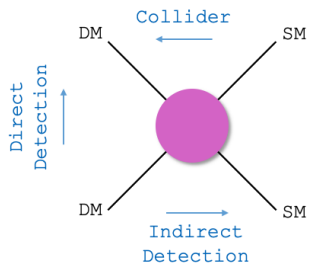

Figure 2.2: Diagram with main processes at collider, direct detection, and indirect detection DM searches.

Indirect Detection

Going from left to right in Fig. 2.2, we have DM annihilations into SM species. If DM particles annihilate into ordinary matter, a measurable signal of photons, neutrinos [81], or cosmic rays can be produced and observed [82]. DM annihilations can also have an impact on the CMB, Big Bang nucleosynthesis (BBN), and the 21-cm Hydrogen line [83], [84].

Direct Detection

Now starting at the bottom and going upwards in Fig. 2.2, we have DM scattering with SM particles in direct detection searches [71], [85], [86]. DM particles from the galaxy can scatter off target particles, electrons or nuclei, in the detector causing a measurable signal.

Accelerator

Finally from right to left in Fig. 2.2, we have searches where the collision of SM particles produces DM or dark sector particles [87]. The largest particle accelerator in the world, the Large Hadron Collider (LHC) searches for BSM physics such as DM [88]. However, since LHC searches are more sensitive to $\gtrsim$ GeV mass DM, this thesis focuses on other lower energy accelerator

experiments better suited as sub-GeV DM searches. These searches can be grouped into invisible and visible searches: where invisible signatures occur when the dark sector particle dominantly decays invisibly to DM, and visible signatures when it dominantly decays to SM species such as electron/positron pairs. In this thesis, we focus on invisible signatures hence models where a dark mediator dominantly decay to DM rather than to SM. The leading experiments include $e^+\,e^-$ colliders, beam dumps, and missing energy or momentum fixed target experiments.

$e^+\,e^-$ colliders search for monophoton signatures, where a dark mediator, A', is produced through the process $e^+e^- \to \gamma A'$. BaBar [89] places the most competitive limits at the moment, and Belle II [90] projected to be the most sensitive in the near future.

At beam dump experiments, a beam of electrons or protons is incident on a target. Interactions between the beam and nuclei of the target lead to the production of dark sector particles. Downstream there is a DM detector which searches for DM-electron or DM-nucleon scattering. Similarly, at fixed target missing momentum/energy experiments, a beam is incident on a target; although instead of searching for DM interactions in a detector, the energy or momentum lost due to the new massive invisible particle is the signal. In Chapter 3 we discuss further and consider these experiments in the context of sub-GeV DM.

2.3 Sub-GeV Dark Matter

If DM is produced thermally in the early universe, i.e. was once in thermal equilibrium with the SM thus produced through freeze-out, its mass can be from $\sim O(\text{MeV})$ to $\sim O(100\text{TeV})$ [68]. The upper mass bound arises mainly because of unitarity violations, and the lower bound from cosmological observations[5]. The experimental efforts in search of nuclear recoils from DM-nuclei scattering, in particular direct detection experiments as described in Section 2.2, are very important for probing GeV - TeV scale DM such as WIMPs. Unfortunately, there is yet to be any discovery of DM at these experiments. With the parameter space of WIMPs (interacting through the SM weak force) shrinking with time, it is natural to consider the possibility that a new gauge boson might mediate potential DM-SM interactions. In this case, DM could be of sub-GeV mass, evading current direct detection experiments. Such light masses do not deposit enough energy via nuclear recoils to be detected. DM-electron scattering however, is a suitable mechanism in which sub-GeV DM particles can be directly discovered. Complimentary to DM-electron scattering at direct detection experiments, accelerator bases searches give strong constraints on sub-GeV DM for many theoretical scenarios [92]. The subject of this thesis is sub-GeV DM models, and considering one of the leading types of experiments for these candidates, fixed target experiments, as a way to measure a potential DM signal.

[5]Energy injection into the SM during BBN is tightly constrained [91].

2.3.1 Dark Photons

If thermal DM has mass below a GeV, there must exist a new type of force, thus gauge boson, mediating the interactions between DM and SM particles. This new gauge boson could be a dark photon, A', arising from a new symmetry, a $U(1)'$, of a dark sector that is neutral under SM forces/gauge groups [93]–[95]. The mechanism responsible for the generation of the mass of this new gauge boson could come from the Stueckelberg mechanism [96] or from an extended Higgs sector. The presence of a new $U(1)'$ symmetry describing a new Abelian[6] gauge boson results in kinetic mixing between the SM photon and the A', a phenomena where the SM photon can change into the A' and vice verse. This gives rise to the following lagrangian [94],

$$\mathscr{L} \supset -\frac{1}{4}F_{\mu\nu}F^{\mu\nu} - \frac{1}{4}F'_{\mu\nu}F'^{\mu\nu} - \frac{\epsilon}{2}F_{\mu\nu}F'^{\mu\nu}, \tag{2.16}$$

where $F_{\mu\nu}$ and $F'_{\mu\nu}$ are the field strength tensors of the SM and dark photons, respectively, and ϵ is the kinetic mixing strength. Diagonalizing the kinetic terms in Equation 2.16 results in the lagrangian for the interaction between SM fermions and the A' (DP) [95],

$$\mathscr{L}_{\text{DP-SM}} \supset -\epsilon e A' q_f \bar{f}\gamma^\mu f, \tag{2.17}$$

where e is the elementary charge, f is the SM fermion spinor, and q_f is their electric charges. I have specifically left out the interaction terms between the A' and the DM, since they are dependent on the nature of the DM particle which is unknown. In Chapter 4, [97] (Paper I) is discussed where we assume a particular DM model thus a particular interaction lagrangian between the A' and DM. Dark photons as a portal to the dark sector are also considered in Chapter 5, [98] (Paper II).

[6] An Abelian theory is one where two successive transformations of the symmetry commute.

Chapter 3

Accelerator Searches

Dark matter that has a mass below a GeV is too light to induce a sizeable nuclear recoil at direct detection experiments. Instead, sub-GeV DM particles can be probed through their electron recoils from direct scattering in an underground detector experiment [85], [99] or at accelerator experiments [92] [100]–[103]. Let us focus on the latter option, where we test for DM signals produced from high energy collisions of SM particles, in particular fixed target experiments rather than LHC experiments. The most relevant current and future experimental constraints on the sub-GeV parameter space, in the case of elastic scalar DM, is shown in Fig. 3.1. Descriptions of the most relevant experiments are given below. Previous studies have focused on the sensitivity on spin-0 and spin-1/2 DM models [104], however other spins are also theoretically viable.

We consider experiments where a high energy beam interacts with nuclei in a target at rest, searches for a mono-energetic ordinary photon from e^+e^- collisions, and briefly discuss visibly decaying dark photon searches.

3.1 Fixed Target Experiments

In these experiments, a relativistic beam of protons or electrons is incident on a fixed target, a piece of material with a high density of protons (high Z) and with zero velocity in the lab frame, causing interactions between the beam and the nuclei of the target as illustrated in Fig. 3.2. Through these interactions, a relativistic flux of dark sector particles could be produced and later detected either through their missing energy/momentum, or directly in a downstream detector. The former we call *missing energy/momentum experiments*, and the latter *beam dump experiments*. The fixed target experiments that we consider are the following:

MiniBooNE: This beam dump experiment searches for electron and nuclear recoils from DM produced in interactions between a 8 GeV proton beam and a steel target [105], [106]. A DM flux can be produced from meson decay, dark bremsstrahlung, and less dominantly through direct parton-level processes; each explained in the following section. This DM flux can be detected from

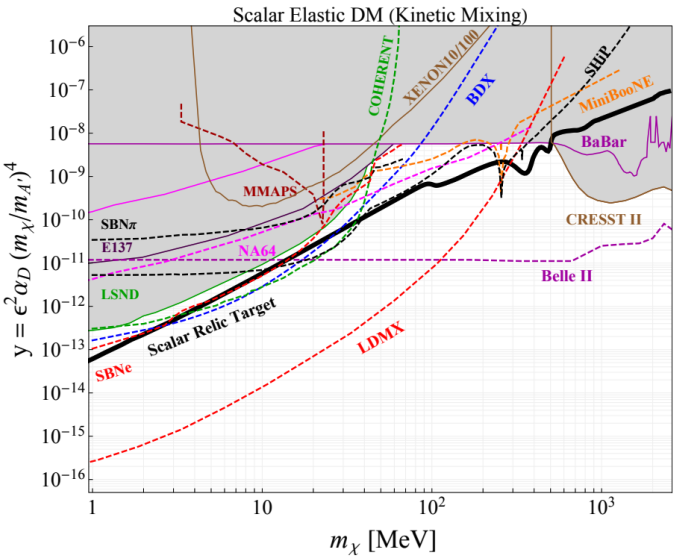

Figure 3.1: Current landscape of current (solid) and future (dashed) experimental constraints on sub-GeV DM [92], in particular the elastic scalar DM with a dark photon mediator. Sensitivity estimates on the parameter y, where $\alpha_D = 0.5$ and $3m_{\rm DM} = m_{A'}$, are plotted as a function of the DM mass.

nuclear and electron recoils in the downstream detector made of mineral oil (CH_3). Zero signal events were measured, thus we draw exclusion limits on the parameter space of various sub-GeV DM models.

LSND: The second beam dump experiment we consider uses an 800 MeV proton beam incident on a water or high atomic number metal target, producing DM mainly through meson decays (the energy is not sufficient for sizeable production through bremsstrahlung) [107]–[109]. Downstream, there is a detector made of mineral oil that is sensitive to DM-electron scattering signals (where the energy is too small to be sensitive to scattering events with nuclei). LSND reported 242 events, which include elastic scattering by neutrinos and potentially DM, with an expected SM background of 229 ± 28.

NA64: This missing energy experiment uses a 100 GeV electron beam with an active target at the CERN SPS [110]. Interactions between the beam electrons and the target nuclei could result in dark photon production through dark bremsstrahlung, followed by its prompt decay to DM or SM states depending on the DM model parameters. Here we mainly focus on the case where $BR_{A'\to \rm DM\,DM} \gg BR_{A'\to \rm SM\,SM}$, thus the A' dominantly decays to DM / invisible final states. In this case, if a dark photon is produced, the recoil electron will receive additional "missing energy", which can be measured in the calorimeters.

LDMX: Currently in the design study phase, LDMX plans to shoot a 4-8

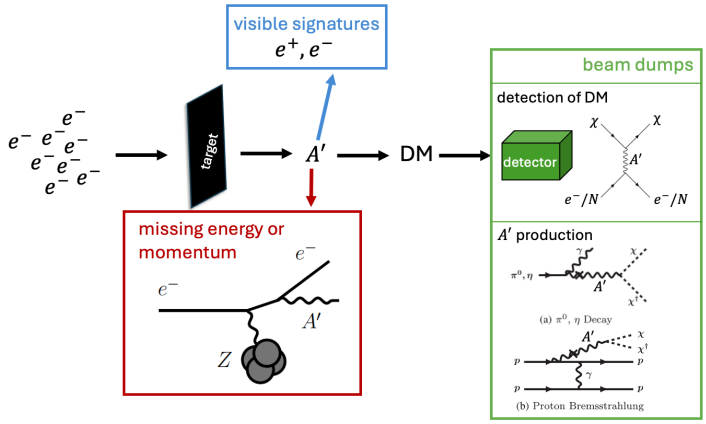

Figure 3.2: Illustration of a fixed target experiment, where an electron (or proton) beam impinges on a fixed target, producing a shower of particles, possibly including dark photons. There are three main types of searches with this set up, missing energy, visible signatures, and beam dumps.

GeV electron beam onto a thin tungsten target, searching for signals from the production of dark photons [104], [111], [112]. Dark photons could be produced through dark bremsstrahlung, and in the case of dominantly invisible decays where $BR_{A' \to \mathrm{DM\,DM}} \gg BR_{A' \to \mathrm{SM\,SM}}$, inducing a measurable transverse momentum kick and missing energy to the recoil electron. The recoil electrons are measured in the detector composed of a tracker, electromagnetic calorimeter, and a hadronic calorimeter. Visible decay signatures can also be measured.

3.1.1 Dark Photon Production

Dark photons can be produced in several ways at fixed target experiments [102], [113]. A flux of neutral mesons, mainly pions and etas, is produced through interactions between protons in a beam and nuclei in the target. In Section 3.1.1.1, DM produced through meson decays is described. Dark photons can also be produced through dark bremsstrahlung, described in Section 3.1.1.2. Direct parton level processes also give rise to dark photon production, but they do not contribute significantly. The contribution of each process, namely the number of elastic nucleon scattering events, is plotted as a function of dark photon mass in Fig. 3.3. Dark bremsstrahlung dominates in the higher mass region $m_{A'} \gtrsim 500$ MeV, while π^0 decay dominates at lower masses.

3.1.1.1 Meson Decay

A proton beam incident on nuclei of a target give rise to the following chain of interactions: $pp \to X\pi^0; \pi^0 \to \gamma A'$, where X denotes an unspecified/unmeasured set of particles and A' can either be on-shell of off-shell. The flux of π^0 (and η if the beam energy is high enough) mesons produced from proton beam target interactions is determined from simulations, and will have a certain distribution

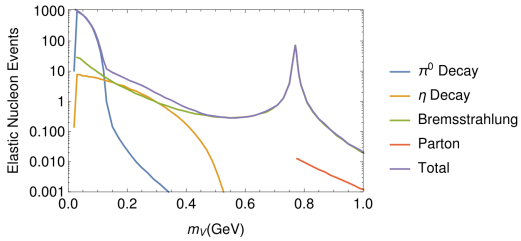

Figure 3.3: Dark photon production channels at proton beam dump experiments [102]. Number of elastic nucleon scattering events as a function of dark photon mass.

in energy [102]. These mesons could then decay to dark photons and after to DM. In the case where $2m_{\rm DM} < m_{A'} < m_{\pi^0}$, the dark photon decays on shell[1] with the branching ratio,

$$BR(\pi^0 \to \gamma\chi\bar{\chi}) = Br(\pi^0 \to \gamma\gamma)2\epsilon^2 \left(1 - \frac{m_{A'}^2}{m_{\pi^0}^2}\right)^3 BR(A' \to \chi\bar{\chi}), \tag{3.1}$$

where DM and its antiparticle are denoted by χ and $\bar{\chi}$. The total number of dark photons produced is then given by,

$$N_{A'} = BR(\pi^0 \to \gamma\chi\bar{\chi}) \times \text{POT} \times N_{\pi^0 \text{per POT}}, \tag{3.2}$$

where POT is the number of protons on target, and $N_{\pi^0 \text{per POT}}$ is the number of pions produced per proton on target, which we approximate here to 1.

3.1.1.2 Dark Bremsstrahlung

Analogous to ordinary photons produced via bremsstrahlung, dark photons can be produced through dark bremsstrahlung, $e^- Z \to e^- Z A'$, where Z is the nucleus in the target, with either electrons or protons depending on the type of beam. The dark photon, A', bremsstrahlung process that we are interested in is,

$$e(p) + Z(P_i) \to e(p') + Z(P_f) + A'(k), \tag{3.3}$$

where the feynman diagrams for this process are drawn in fig. 3.4. See [114] for amplitude expressions. The integral over phase space is not easy to compute, therefore the Weizsacker-Williams approximation can be used to compute the cross section of dark bremsstrahlung [115], [116].

3.1.2 Simulations

In this thesis, we use a modified version of BdNMC [102], a Monte Carlo simulation software for modeling production, propagation, and scattering in

[1]We will restrict ourselves to the on-shell case in this thesis, but in the off-shell case the branching ratio involves a phase space integral that must be solved numerically, since the narrow width approximation no longer holds [113].

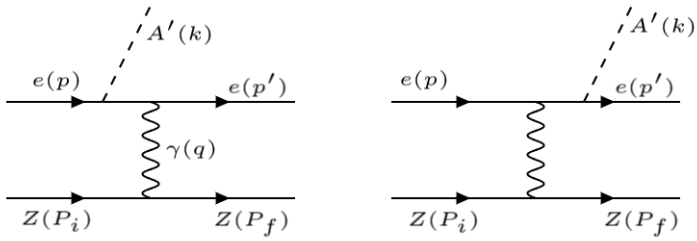

Figure 3.4: Dark photon bremsstrahlung feynman diagrams where a high energy electron, e, is incident on a target, Z.

beam dump experiments. BDNMC first simulates the production of dark photons from bremsstrahlung and meson decays, considering both on and off-shell contributions. Next it models the scattering of the produced DM inside the detector with nucleons and electrons, taking into account the detector material and geometry. In this work, additional DM models, such as dirac fermion DM and various vector DM models, were added to the software. This involves computing and adding the DM-electron and DM-nucleon cross section and branching ratios for the DM models of interest to the software.

For simulation of the future experiment LDMX, the matrix element generator software MadGraph [117], is used as a way to approximate the expected dark bremsstrahlung signal. The software is used with UFO (universal feynman output) [118] files as input, which include the new vertices associated with the dark photon and dark matter, along with an approximation of the tungsten and its interaction with an ordinary photon. In this thesis, we consider a dark photon with vector couplings to electrons/positrons. The tungsten nucleus is crudely approximated as a heavy fermion with a charge if 74, with a vector coupling to the photon with the following form factor [119],

$$G(t) = \left(\frac{a^2 t}{1+a^2 t}\right)^2 \left(\frac{1}{1+t/d}\right)^2 Z^2 + \left(\frac{a'^2 t}{1+a'^2 t}\right)^2 \left(\frac{1+\frac{t}{4m_p^2}(\mu_p^2-1)}{\left(1+\frac{t}{0.71\ \mathrm{GeV}^2}\right)^4}\right)^2 Z, \tag{3.4}$$

where $t \equiv -q^2$, q is the momentum of the photon, $a = 111 Z^{-1/3}/m_e$ where Z is the atomic number of the nucleus, $d = 0.164\ \mathrm{GeV}^2 A^{-2/3}$ where A is the atomic mass of the nucleus, $a' = 773 Z^{-2/3}/m_e$, m_p is the proton mass, and $\mu_p = 2.79$. The first term is the elastic component, while the second is the inelastic component. Using this, the dark photon bremsstrahlung events are simulated using Madgraph at various dark photon masses. The production of dark photons at LDMX would result in additional transverse momentum along with missing energy of the recoil electron. The energy, E, and transverse momentum, $|p_T|$, distributions of the recoil electron are plotted in Fig. 3.5 [112].

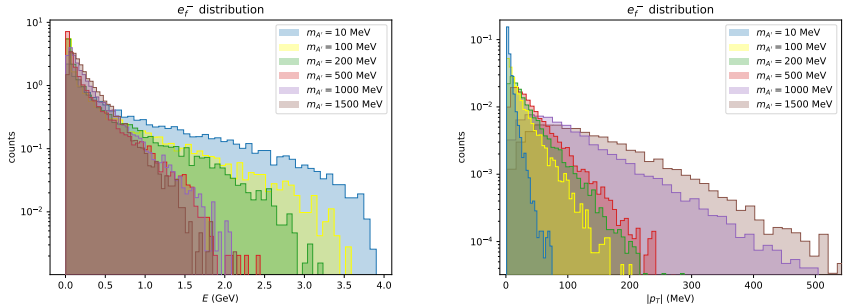

Figure 3.5: Kinematic distributions of the recoil electron from dark bremsstrahlung at LDMX at varying dark photon masses, simulated using Madgraph [112].

3.2 Mono-Photon Searches

Electron positron collisions could produce dark photons through the process $e^+e^- \to \gamma A'$. If the dark photon dominantly decays to DM rather than to visible states, the signal is a monochromatic single photon along with missing energy and momentum. The production of dark photons would result in a peak in the missing mass spectrum, $m_X^2 = s - 2E_\gamma^*\sqrt{s}$, where s is the center of mass (CM) energy squared and E_γ^* is the energy of the photon in the CM frame. We consider in Papers I and II the results from the BaBar collaboration [89] and the future sensitivity projections of Belle-II [90].

3.3 Visibly Decaying Dark Photon Searches

If we consider dark photons that significantly decay to visible states, such as e^+ e^-, these final states can be detected [93]. In collider experiments, a resonance in the invariant mass distribution would constitute a dark photon signal. Beam dump experiments search for downstream visible decay products from dark photons produced through dark bremsstrahlung. In this thesis, we will remain in the parameter space where the dark photon dominantly decays invisible, thus we will not consider visible signatures.

Chapter 4

Spin-1 Sub-GeV Dark Matter

The realm of currently possible theoretical explanations of DM is overwhelming and infinite. As discussed in Section 2.1, existing literature explores many theoretical models describing DM's nature, and within the literature for sub-GeV DM with a dark photon mediator only spin-0 and spin-1/2 DM models have been explored. DM could also be a new spin-1 boson, X, which interacts with SM particles through another new spin-1 particle mediator (such as the dark photon), or even through multiple mediators [85], [97], [120]. These mediators, being the paricle responsible for interactions between DM particles and electrically charged SM species, could potentially be observed at various experiments, in particular fixed target experiments.

The aim of Paper I within this thesis is to extend these studies on sub-GeV DM models which can be probed by current and future fixed target experiments, to include spin-1 DM models. We first study a set of simplified spin-1 DM models which are directly comparable to previously studied DM models. These models are subject to strong unitarity violations, therefore this motivates us to consider a renormalizable UV complete spin-1 model which includes an extended Higgs sector. We study the phenomenology of these models, determining the experimental sensitivity and regions of parameter space consistent with the observed relic density [13]. This chapter is based on [97] , where we refer to Paper I in Part II for the details. In this chapter, the necessary background and main conclusions of this work are discussed.

4.1 Simplified Models

The underlying nature of the constituents of matter, particles, are described by a lagrangian density, $\mathscr{L}$, representing the particles of the theory and their interactions. Simplified models are theories which minimally extend the SM such that they can be studied in the context of experimental searches [121]. Unlike effective field theories, simplified models include a particle mediator between

the visible and dark sectors. However, they still neglect UV-completeness and possibly also a mass giving mechanism that a complete theory would include – thus additional fields and interactions are being neglected.

We extend the SM with one complex vector field X^μ and one real vector field A'^μ, where the first is the DM and the second is the mediator [122] arising from a new $U(1)'$ gauge group. The simplicity of this extension allows for direct comparison between scalar and fermionic DM models which have already been investigated in the literature. Writing down the most general lagrangian describing the interactions between X^μ and A'^μ gives,

$$\begin{aligned}\mathscr{L} \supset & -\left[ib_5 X^\dagger_\nu \partial_\mu X^\nu A'^\mu + b_6 X^\dagger_\mu \partial^\mu X_\nu A'^\nu + \text{h.c.}\right] \\ & -\left[b_7 \epsilon_{\mu\nu\rho\sigma}\left(X^{\dagger\mu}\partial^\nu X^\rho\right) A'^\sigma + \text{h.c.}\right] \\ & - e\epsilon {A'}_\mu \bar{f}\gamma^\mu f,\end{aligned} \tag{4.1}$$

where b_i are the dark sector couplings, ϵ is the kinetic mixing strength, e is the elementary charge, and f is the SM fermion field which includes electrons, muons, taus, and quarks, and does not include neutrinos. The dark sector couplings, without loss of generality, are such that b_5 can be taken to be real, while b_6 and b_7 complex. The first and second lines of Equation 4.1 can arise in models where X^μ is part of a non-abelian and abelian field theory, respectively. The third line describes the interaction between the A' and the SM fermions arising from the kinetic mixing, as described in Section 2.3.1. We consider the cases where only one of the b_i couplings are non-zero, and ϵ is always a non-zero free parameter of the model. To facilitate easy comparison between other DM models considered in previous literature, we label the dark coupling as g_D, where g_D is one of b_5, $\Re[b_6]$, $\Im[b_6]$, $\Re[b_7]$, or $\Im[b_7]$, and $\alpha_D \equiv \frac{g_D^2}{4\pi}$. $\alpha_D = 0.5$ throughout this chapter and Paper I.

4.1.1 Violations of Perturbative Unitarity

By imposing conservation of probability in quantum mechanics, the S matrix must be unitary, $S^\dagger S = 1$. From this, it follows that a bound arises on the partial wave amplitudes, $\mathcal{M}^J_{if}$, which are scattering amplitudes with fixed total angular momentum J. For example, we consider the process $i_1 i_2 \to f_1 f_2$, where the following bounds come from the unitarity condition [123],

$$\begin{aligned} & 0 \leq \Im(\mathcal{M}^J_{ii}) \leq 1 \\ & |\Re(\mathcal{M}^J_{ii})| \leq \frac{1}{2}, \end{aligned} \tag{4.2}$$

where $\mathcal{M}^J_{if}$ is the diagonalized matrix of matrix of elements of all possible 2 particle states, and $\mathcal{M}^J_{ii}$ are the eigenvalues [124], [125]. For a given theory, if this *unitarity bound* is violated in any process at tree level (leading order in perturbation theory), this signifies the necessity of either including higher order terms (perturbativity has broken down) or that the theory requires additional fields - each of which could restore unitarity. The former case arises for incomplete theories such as effective field theories and simplified

models at high scattering energies, couplings, or for particular masses. Due to our simplified spin-1 DM models having momentum dependence introduced from the vertices and from the longitudinal component of the polarization vectors, our simplified models violate unitarity at certain scattering energies. We consider violations of unitarity from DM self scattering [126] and DM-e^- scattering.

Figures 4 and 5 of Paper I [97] show the resulting calculated unitarity "bound", or region of theoretical validity of the simplified model. This bound is strong at relevant energies, and even stronger and higher energies, highlighting the UV (ultraviolet) incompleteness of the theory.

4.2 Non-Abelian SIMPs

With motivation to avoid unwanted unitarity violations as described in the previous section, we consider a second, more complete model for spin-1 DM where the SM is extended by a local $SU(2)_X \times U(1)_{Z'}$ symmetry group in which the SM species are not charged under [127]. In this model, DM is a Strongly Interacting Massive Particle (SIMP), characterized by the $3 \to 2$ annihilations of the DM in the early universe setting the relic density. This leads to strong couplings in the dark sector for setting the relic density, but weaker couplings with the SM species which can evade current experimental constraints. It was found in the work [128], that SIMPs can achieve the correct relic density with masses ~ 0.1 GeV. We can also have SIMPs that are spin-1 DM candidates [129].

This model includes an extended Higgs sector with a scalar singlet, S, and a scalar H_X which can take several representations under $SU(2)_X$. The gauge bosons associated with the new $SU(2)_X$ symmetry are $X_{\mu,i}$ $(i = 1, 2, 3)$, or equivalently $X_\mu \equiv (X_{\mu,1} + iX_{\mu,2})/\sqrt{2}$ and $X_\mu^\dagger \equiv (X_{\mu,1} - iX_{\mu,2})/\sqrt{2}$, and with $U(1)_{Z'}$, Z'_μ. The vacuum expectation values (VEVs), v_S and v_X, of the dark scalars, S and H_X respectively, spontaneously break the $SU(2)_X \times U(1)_{Z'}$ symmetry, giving the dark gauge bosons mass and combining $X_{\mu,1}$ and $X_{\mu,2}$ to give the complex gauge boson X_μ, the DM candidate, and generating two linear combinations of Z'_μ and $X_{3,\mu}$ which we denote by $\tilde{Z}'_\mu$ and $\tilde{X}_{3,\mu}$.

A gauge kinetic mixing is introduced, leading to interactions between $\tilde{Z}'$, $\tilde{X}_3$, and SM fermions. Due to v_X, $\tilde{X}_{\mu,3}$ has a different mass from X_μ, therefore there are two mediators between the dark and visible sectors, the $\tilde{Z}'$ (analgous to the dark photon) and the $\tilde{X}_3$.

By construction this model is not subject to the unitarity violations de-

scribed in the previous section. The interaction lagrangian is given by,

$$\begin{aligned}\mathscr{L} \supset & -ig_X \cos\theta'_X \left[\left(\partial^\mu X^\nu - \partial^\nu X^\mu\right) X^\dagger_\mu \tilde{X}_{3,\nu} - \left(\partial^\mu X^{\nu\dagger} - \partial^\nu X^{\mu\dagger}\right) X_\mu \tilde{X}_{3,\nu} \right. \\ & \left. + X_\mu X^\dagger_\nu \left(\partial^\mu \tilde{X}_3^\nu - \partial^\nu \tilde{X}_3^\mu\right) \right] \\ & - ig_X \sin\theta'_X \left[\left(\partial^\mu X^\nu - \partial^\nu X^\mu\right) X^\dagger_\mu \tilde{Z}'_\nu - \left(\partial^\mu X^{\nu\dagger} - \partial^\nu X^{\mu\dagger}\right) X_\mu \tilde{Z}'_\nu \right. \\ & \left. + X_\mu X^\dagger_\nu \left(\partial^\mu \tilde{Z}'^\nu - \partial^\nu \tilde{Z}'^\mu\right) \right] \\ & - e\varepsilon \cos(\theta'_X)\, \tilde{Z}'_\mu\, \bar{f}\gamma^\mu f + e\varepsilon \sin(\theta'_X)\, \tilde{X}_{3\mu}\, \bar{f}\gamma^\mu f,\end{aligned}$$

where $\tan(2\theta'_X) = \frac{2\cos\theta_X \sin\theta_X}{\cos\theta_X^2 - \alpha \sin\theta_X^2}$, $\sin\theta_X = \frac{g_{Z'}}{\sqrt{g_X^2 + g_{Z'}^2}}$. We take $\theta'_X \ll 1$, therefore Z's are dominantly produced in dark bremsstrahlung events at fixed target experiments. Similarily to the simplified spin-1 DM models, we set $\frac{g_X^2}{4\pi} = 0.5$ such that the dark sector coupling is much larger than the SM coupling ϵe.

4.2.1 SIMP Relic Density

With sufficient couplings between the SM fermions and the dark sector, DM would have once been in thermal equilibrium with the SM bath – leading to the freeze-out mechanism for DM production. The dominant DM annihilation processes are $X^+X^-X^+ \to X^+\tilde{X}_3$ and the so called forbidden annihilation $X^+X^- \to \tilde{X}_3\tilde{X}_3$, where the former is dominant if $1 < m_{\tilde{X}_3}/m_X < 2$, and the latter if $m_{\tilde{X}_3}/m_X < 1$. This is in contrast to s-channel DM annihilation to SM fermions through $\tilde{X}_3$, which is suppressed since $g_X \gg \epsilon e$. This leaves the relic density contours, or so called *thermal targets* independent of ϵ, only varying with the dark coupling and the masses.

However, we must be careful to check whether DM and the $\tilde{X}_3$ remain in kinetic equilibrium with the SM during freeze-out; otherwise structure formation constraints are not satisfied. DM is easily able to stay in kinetic equilibrium through elastic scattering between DM and $\tilde{X}_3$, given that $\tilde{X}_3$ remains in kinetic equilibrium, since g_X is large. $\tilde{X}_3$, through its decays to SM species, is able to stay in equilibrium with the SM. We impose that,

$$n_{\tilde{X}_3,\mathrm{eq}}(T_f)\Gamma_{\tilde{X}_3} > H(T_f) n_{X,\mathrm{eq}}(T_f)\,, \tag{4.3}$$

where $H(T_f)$ is the Hubble rate at the freeze-out temperature T_f, and the equilibrium number density of a species i is given by,

$$n_{i,\mathrm{eq}}(T) = \frac{45 m_i^2}{2T^2 g_{*s}(T)\pi^4} s K_2(m_i/T), \tag{4.4}$$

where s is the entropy density, $g_{*s}(T)$ is the effective number of entropic relativistic degrees of freedom at the temperature T, K_2 is a modified Bessel function of the second kind. In Equation 4.3, $\Gamma_{\tilde{X}_3}$ is the total decay rate of $\tilde{X}_3$, for which the expression is given in [127].

We consider the particular choice of parameters where $m_{\tilde{X}_3}/m_X \approx 2$, such that the $3 \to 2$ process is dominant. There is a resonance in the $3 \to 2$ cross

section when $m_{\tilde{X}_3}/m_X \approx 2$, therefore the relic density drops to zero as the ratio approaches 2 from the left. Since the cross section is inversely proportional to the DM mass, larger DM masses give larger relic densities. However, as long as the DM mass is sufficient, very close to the resonance the relic density will be in agreement with Planck measurements [13]. The relic density is also independent of ϵ since the annihilation process only contains dark sector particles. Therefore, there is an entire region in ϵ vs m_X parameter space consistent with the correct relic density, and for lighter masses the DM could be a sub-component.

4.3 Thermal Targets

We compare the thermal targets of scalar, psuedo-dirac, majorana, and vector DM (simplified $\Re[b_5]$ and SIMP) in Fig. 4.1. These thermal targets are plotted as a function of $y = \epsilon^2 \alpha_D \left(\frac{m_X}{m_{A'}}\right)^4$ and m_X, with approximate current experimental limits[1] in blue and relevant future projections as dashed curves. As described

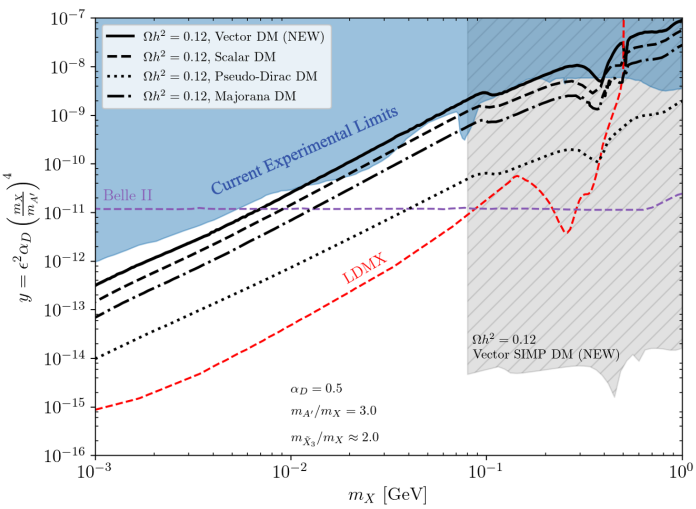

Figure 4.1: Thermal targets (black lines representing the parameters which reproduce the observed relic density [13]) as a function of $y = \epsilon^2 \alpha_D \left(\frac{m_X}{m_{A'}}\right)^4$ and m_X, for various DM models.

in detail in Paper II, we find that certain simplified spin-1 DM models are the first models to be probed by upcoming results from NA64 and the future experiment LDMX. Furthermore, the spin-1 SIMP models, having a large viable parameter space, will be probed by LDMX. We have shown that the

[1] Some of these limits are DM model dependent, for example when they involve DM scattering in a detector. For simplicity, we take these limits for complex scalar DM as an approximate benchmark of the current experimental status in this plot.

theoretical landscape of future accelerator experiments such as LDMX is rich with viable DM scenarios.

Chapter 5

Global Fits

Throughout this thesis and in Paper I, we have been considering several observations that each lead to constraints on our DM models by the absence of any events attributed to DM. The conventional way of determining excluded regions of the parameter space is to draw separate exclusion limits at a given confidence level for each experiment/observation. The rate at which the parameter value is falsely excluded for one experiment is given by $1 - \mathrm{CL}$, where CL is taken commonly in particle physics to be 90% or 0.9. However when combining multiple experiments, this "patching" of exclusion limits results in a false reporting of the confidence level. The actual error is $1 - \mathrm{CL}^N$, where N is the number of experiments [130]. For a $\mathrm{CL} = 0.9$ and 3 experimental constraints, the error is then $1 - 0.9^3 \approx 0.27$, a larger error than the 0.1 that one could naively expect.

In addition to the desire for a more statistically robust method of handling multiple experimental constraints, the large parameter space that comes with many DM models can be non-trivial to navigate. In particular, making statements about the regions of parameter space still unexcluded by current data is a multidimensional problem. The suggestion is to instead perform so called *global fits* of the parameter space, where the likelihoods of many constraints are combined in a statistically robust framework. This chapter is based on the work of paper II found in Part II [98].

5.1 Combining Likelihoods

When performing global fits, we consider the total likelihood, or probability of the data given the model and nuisance parameters, which is simply the product of every relevant likelihood,

$$\mathcal{L}_{\text{total}} = \mathcal{L}_{\text{DD}} \times \mathcal{L}_{\text{collider}} \times \mathcal{L}_{\text{ID}} \times \mathcal{L}_{\text{cosmology}} \times \cdots \tag{5.1}$$

such as the likelihood from direct detection, collider, indirect detection, and cosmology, which we take to be independent of each other. Depending on the statistical nature of the experiment or observation, the likelihood will take

a certain form. For example, the likelihood for a counting experiment such as direct detection and accelerator experiments takes the form of a Poisson distribution, where for n events is,

$$\mathcal{L} = e^{-(s+b)} \frac{(s+b)^n}{n!}, \tag{5.2}$$

where s is the number of signal events predicted from theoretical simulations/calculations and b is the number of expected events from known background processes.

5.1.1 GAMBIT

GAMBIT v2.5.0 is a publicly available software package which performs global fits on DM models, with the goal of being flexible and extendable to other particle physics models and likelihood analyses. [131]. Within GAMBIT exists a growing number of likelihoods categorized into modules, that can all be analyzed at once in the context of a particular DM model. Within these modules there are different analyses involving backends to simulation and calculation software with varying levels of complexity. In particular interest to this work, the ColliderBit module calculates high energy collider physics observables [132].

5.2 Sub-GeV Dark Matter Analysis

With the many existing and future probes of sub-GeV DM, each dominating in their own region of parameter space in a complimentary way, global fits are able to provide us with a status update on this class of DM candidates. We determine the viable regions of parameter space that are not already ruled out by experiments and observations, and compare them to projections of future experiments. In particular, we consider two theoretical scenarios: a complex scalar Φ and a Dirac fermion ψ. DM each interacting with SM through a dark photon A' portal as described in Section 2.3.1, with the following lagrangians,

$$\mathcal{L}_\Phi = |\partial_\mu \Phi|^2 - m_{\rm DM}^2 |\Phi|^2 + i g_{\rm DM} A'^\mu \left[\Phi^* (\partial_\mu \Phi) - (\partial_\mu \Phi^*)\Phi\right] - g_{\rm DM}^2 A'_\mu A'^\mu |\Phi|^2, \tag{5.3}$$

$$\mathcal{L}_\psi = \bar{\psi}(i\partial\!\!\!/ - m_{\rm DM})\psi + g_{\rm DM} A'^\mu \bar{\psi}\gamma_\mu \psi, \tag{5.4}$$

where $L_{\text{DP-SM}}$ from Equation 2.17 describes the A'-SM fermion interaction for both scenarios. We consider the case where DM has a mass from 1 MeV to 1 GeV and $2m_{\rm DM} \leq m_{A'}$, therefore dark decays of the A' are allowed and dark bremsstrahlung occurs on-shell. We allow for an asymmetry between the number of DM particles and anti-DM particles by letting $\eta_{\rm DM} \equiv \frac{n_\chi - n_{\bar{\chi}}}{s}$ be different from 0, where s is the entropy density and n_χ is the DM number density.

DM annihilations to SM species would inject energy into the photon-baryon plasma, leading to deviations in what is measured of the CMB. Limits on this exotic energy injection are placed on the DM annihilation cross section. In

addition, DM in our galaxy could produce so called secondary signals; from annihilating and producing electron positron pairs which, via inverse compton scattering, would upscatter low energy photons producing X-rays which can be measured with telescopes [133]. Certain sub-GeV DM models are subject to strong constraints from these X-ray measurements, in particular for Dirac fermion DM where the non-relativistic thermally averaged cross section, $\langle \sigma v \rangle$[1], for DM annihilation to SM through the dark photon mediator is independent of the velocity. This leaves a large part of the parameter space excluded, including parts where the relic density constraint is satisfied. However, $\langle \sigma v \rangle \sim v^2$ for a complex scalar DM, leading to much weaker constraints from CMB and X-ray measurements.

We explore three ways in which these tight constraints on Dirac fermion DM can be relaxed, evading indirect detection. The first way is through resonant enhancement of the annihilation cross section during freeze-out, which occurs if $2m_{\rm DM} \sim m_{A'}$. If DM freezes-out at the time/temperature at which there is a resonance in $\langle \sigma v \rangle$, more DM annihilations will occur before freezing-out, leading to an overall smaller abundance - thus smaller couplings are required to reproduce the observed abundance. We define the resonance parameter $\epsilon_R \equiv \frac{m_{A'}^2 - 4m_{\rm DM}^2}{4m_{\rm DM}^2}$ to parameterize the closeness to resonance. The next way is through an asymmetry of DM to anti-DM; if $\eta_{\rm DM} > 0$. These leads to a supression of the expected indirect detection signals since only the symmetric component can annihilate. The last way to relax the strong constraints is if the considered DM particle only constitutes a portion of the DM abundance, if the relative abundance, $f_{\rm DM} \equiv \frac{\Omega_{\rm DM} h^2}{\Omega_{\rm DM,obs} h^2} < 1$, namely sub-component DM.

For both DM models, we combine constraints from cosmology, astrophysics, accelerators, and direct detection experiments in both frequentist and bayesian analyses. In Fig. 5.1, the profile likelihood from the frequentist analysis is plotted as a function of kinetic mixing κ and dark photon mass $m_{A'}$, with the $1-\sigma$ (68% confidence level) and $2-\sigma$ (95 % confidence level) contours shaded in blue, and the best fit point represented by a star. Low dark photon masses are not preferred due to the cosmological likelihoods. In particular, observations of light element abundances constrain the amount in which Big Bang Nucleosynthesis can be altered by a beyond the SM species. When the A' is too light, it decouples from the thermal bath too light, contributing too long to the energy density and hence the number of effective degrees of freedom. Large couplings are excluded by fixed target experiments, most dominantly NA64. The positively sloped shape of the $1-\sigma$ contour comes from the inversely proportionality of $m_{A'}$ with the number of expected events at fixed target experiments, with flattening at $\sim$ 1GeV possibly attributed to the BaBar experiment. Below a certain κ, DM would be overproduced in the universe inconsistent with Planck measurements.

Projections of the future experiments LDMX, described in Section 3.1,

[1]The thermally averaged annihilation cross section in the non-relativistic limit can be expanded in powers of v^2 in a partial-wave expansion $\langle \sigma v \rangle \approx a + bv^2 + \cdots$, where a is the s-wave term, b the p-wave, etc. The spin of the incoming and outgoing particles can forbid certain terms due to conservation of angular momentum. For scalar DM, s-wave annihilations through an s-channel A' are forbidden, leading to p-wave or v^2 dependent annihilations.

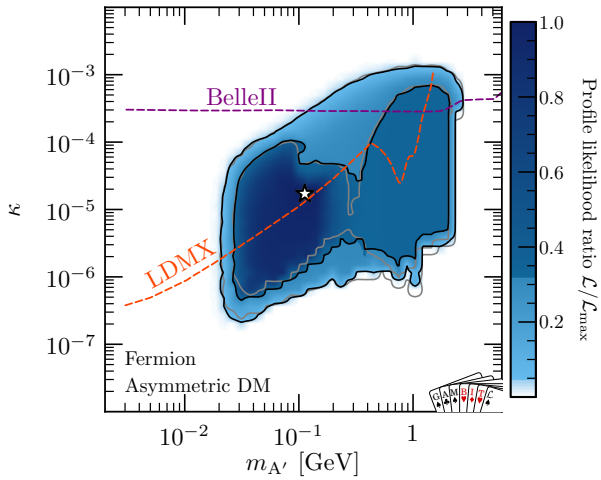

Figure 5.1: Profile likelihood ratio of Dirac fermion DM as a function of kinetic mixing parameter κ and the A' mass, with 1-σ and 2-σ confidence regions drawn in black and shaded in blue for $\Omega h^2 \approx 0.12$, and in grey for $\Omega h^2 < 0.12$ (subcomponent DM). Here we allow for an asymmetry in the DM to anti-DM abundance. The star indicates the best-fit. The expected exclusion bound from the future experiments LDMX and Belle-II are drawn in dashed red and purple, respectively. Taken from Paper II [98].

and Belle-II are drawn as dashed curves, demonstrating the large sensitivity potential. LDMX is expected to probe 64% of the posterior volume.

Bayesian analyses are also given in Paper II, where the main difference is that finely tuned parameters are penalised and instead parameters which can fit observations in large areas of parameter space are favoured.

Chapter 6

Summary and Outlook

With the observational evidence for the existence of a new type of matter in abundance, we work towards identifying its nature. This thesis has outlined a motivation for the existence of BSM physics which explains the mysterious nature of DM, in particular a new particle. The lack of our current understanding of DM and its particle nature leaves us with a vast range of possible properties this matter could be described by such as its mass, spin, coupling to other particle species, and mechanism for production. That being said, it is reasonable to assume that DM was once in thermal equilibrium with the rest of the species in one thermal bath in the early universe. Given this assumption, the possibilities are reduced due to a more narrow mass window, where it is bounded from below from observations of BBN and from above due to unitarity violations. This thermal window can be segmented into two regions: WIMPs and Sub-GeV DM, in the $m_{\mathrm{DM}} >$ GeV and $m_{\mathrm{DM}} <$ GeV mass windows respectively. This thesis focuses on the latter mass window, where the mass is too light to induce sizeable nuclear recoils in direct detection experiments.

Sub-GeV DM is less explored experimentally than WIMPs, however there are a growing number of searches dedicated to this mass regime. Among them, fixed target experiments at particle accelerators, for a large pool of theoretical scenarios, are the best experimental probes. We have investigated the particular scenario where DM is a complex vector field of spin-1, extending the theoretical landscape of models considered in the context of fixed target experiments. We consider two theoretical frameworks: simplified and SIMP models, the former being easily comparable to previously considered models but with unitarity violations at certain energies, and the latter a more complete model not subject to these unitarity violations but with a different process in the early universe setting the relic abundance. We demonstrate that certain spin-1 DM models are the first models to be probed by upcoming experiments in both frameworks.

Sub-GeV DM models are subject to several constraints from cosmology, astrophysical observations, and laboratory experiments. In contrast to conventional approaches to studying the many constraints on a model, global fits are statistically robust and provide an easier method to scan the parameter

space for preferred and excluded regions. We implement new likelihoods of each relevant constraint into the software GAMBIT and perform global fits considering all relevant constraints of two benchmark DM models, a complex scalar and a Dirac fermion, each with a dark photon mediator. The Dirac fermion DM in particular is subject to strong constraints from indirect detection, but including an asymmetry parameter and/or allowing for the DM to be subcomponent relaxes these constraints.

The story does not end here. In fact, there are ongoing efforts to extend the work discussed in this thesis in various ways. Firstly, we are considering another spin-1 DM model arising from an extended Higgs sector where the SM is extended by a new $SU(2)_{\rm dark}$ symmetry, without a new $U(1)'$. In this scenario, the mass hierarchy between the dark photon and the DM is reversed, such that $m_{A'} < m_{\rm DM}$. This leads to interesting phenomenology at fixed target experiments complimentary to the reversed mass hierarchy case, since invisible dark photon production occurs off-shell and the dark photon decays visibly. Secondly, there is ongoing work with extended dark photon models and their corresponding signatures at LDMX. These models have dark magnetic dipole moment interaction terms between the dark photon and SM fermions. The different structure of these interaction terms leads to different expected kinematic distributions at missing momentum experiment LDMX, in addition to different sensitivities at other experiments. Next, the complementarity between different experiments has been an important aspect of both papers, but in particular in Paper II [98]. If an experiment such as a missing momentum experiment (LDMX for example) were to measure a signal, since it is not directly probing DM, the signal would still need to be validated at some experiment that directly probes the DM. For a set of different direct detection experiments, we determine the level of exposure required to measure or exclude this hypothesis at a chosen confidence level. Finally, the current working method of the LDMX collaboration to perform sensitivity estimates and analyses with the data that will come in the future does not use the full kinematic spectral information. We hypothesize that taking into account the energy and transverse momenta information will lead to stronger sensitivities. To explore this hypothesis, we are currently developing a likelihood-based statistical framework for the analysis of future LDMX data and sensitivity projections.

Bibliography

[1] R. S. Westman, "Book review: "de revolutionibus" in english, copernicus: On the revolutions of the heavenly spheres," *Journal for the History of Astronomy*, vol. 8, no. 2, pp. 145–147, 1977. DOI: 10.1177/002182867700800210. eprint: https://doi.org/10.1177/002182867700800210. [Online]. Available: https://doi.org/10.1177/002182867700800210 (cit. on p. 3).

[2] I. Newton, *Philosophiae Naturalis Principia Mathematica*. 1687. DOI: 10.3931/e-rara-440 (cit. on p. 3).

[3] M. S. Longair, *The Cosmic Century: A History of Astrophysics and Cosmology*. Cambridge University Press, 2006. DOI: 10.1017/CBO9781139878319 (cit. on p. 3).

[4] A. Einstein, "The foundation of the general theory of relativity," 1916 (cit. on p. 4).

[5] A. Einstein, "On the electrodynamics of moving bodies," *Annalen Phys.*, vol. 17, pp. 891–921, 1905. DOI: 10.1002/andp.200590006 (cit. on p. 4).

[6] M. Milgrom, "A Modification of the Newtonian dynamics as a possible alternative to the hidden mass hypothesis," *Astrophys. J.*, vol. 270, pp. 365–370, 1983. DOI: 10.1086/161130 (cit. on pp. 4, 13).

[7] A. Einstein, "Cosmological Considerations in the General Theory of Relativity," *Sitzungsber. Preuss. Akad. Wiss. Berlin (Math. Phys.)*, vol. 1917, pp. 142–152, 1917 (cit. on p. 4).

[8] E. Hubble, "A relation between distance and radial velocity among extra-galactic nebulae," *Proc. Nat. Acad. Sci.*, vol. 15, pp. 168–173, 1929. DOI: 10.1073/pnas.15.3.168 (cit. on p. 4).

[9] G. Lemaitre, "Republication of: The beginning of the world from the point of view of quantum theory," *Nature*, vol. 127, p. 706, 1931. DOI: 10.1007/s10714-011-1214-6 (cit. on p. 4).

[10] G. Lemaitre, "The expanding universe," *Annales Soc. Sci. Bruxelles A*, vol. 53, pp. 51–85, 1933. DOI: 10.1023/A:1018855621348 (cit. on p. 4).

[11] A. G. Riess *et al.*, "Observational evidence from supernovae for an accelerating universe and a cosmological constant," *Astron. J.*, vol. 116, pp. 1009–1038, 1998. DOI: 10.1086/300499. arXiv: astro-ph/9805201 (cit. on p. 4).

[12] S. Perlmutter *et al.*, "Measurements of Ω and Λ from 42 high redshift supernovae," *Astrophys. J.*, vol. 517, pp. 565–586, 1999. DOI: 10.1086/307221. arXiv: astro-ph/9812133 (cit. on p. 4).

[13] N. Aghanim *et al.*, "Planck 2018 results. VI. Cosmological parameters," *Astron. Astrophys.*, vol. 641, A6, 2020, [Erratum: Astron.Astrophys. 652, C4 (2021)]. DOI: 10.1051/0004-6361/201833910. arXiv: 1807.06209 [astro-ph.CO] (cit. on pp. 5, 11–14, 27, 31).

[14] R. A. Alpher and R. Herman, "Evolution of the Universe," *Nature*, vol. 162, no. 4124, pp. 774–775, 1948. DOI: 10.1038/162774b0 (cit. on p. 5).

[15] R. A. Alpher and R. C. Herman, "Remarks on the Evolution of the Expanding Universe," *Phys. Rev.*, vol. 75, no. 7, pp. 1089–1095, 1949. DOI: 10.1103/physrev.75.1089 (cit. on p. 5).

[16] R. A. Alpher and R. Herman, "REFLECTIONS ON EARLY WORK ON 'BIG BANG' COSMOLOGY," *Phys. Today*, vol. 41N8, pp. 24–34, 1988. DOI: 10.1063/1.881126 (cit. on p. 5).

[17] A. A. Penzias and R. W. Wilson, "A Measurement of excess antenna temperature at 4080-Mc/s," *Astrophys. J.*, vol. 142, pp. 419–421, 1965. DOI: 10.1086/148307 (cit. on p. 5).

[18] R. H. Dicke, P. J. E. Peebles, P. G. Roll and D. T. Wilkinson, "Cosmic Black-Body Radiation," *Astrophys. J.*, vol. 142, pp. 414–419, 1965. DOI: 10.1086/148306 (cit. on p. 5).

[19] W. Heisenberg, "A quantum-theoretical reinterpretation of kinematic and mechanical relations," *Z. Phys.*, vol. 33, pp. 879–893, 1925. DOI: 10.1007/BF01328377 (cit. on p. 6).

[20] E. Schrödinger, "Quantisierung als Eigenwertproblem," *Annalen Phys.*, vol. 384, no. 4, pp. 361–376, 1926. DOI: 10.1002/andp.19263840404 (cit. on p. 6).

[21] G. Aad *et al.*, "Observation of a new particle in the search for the Standard Model Higgs boson with the ATLAS detector at the LHC," *Phys. Lett. B*, vol. 716, pp. 1–29, 2012. DOI: 10.1016/j.physletb.2012.08.020. arXiv: 1207.7214 [hep-ex] (cit. on p. 7).

[22] S. Chatrchyan *et al.*, "Observation of a New Boson at a Mass of 125 GeV with the CMS Experiment at the LHC," *Phys. Lett. B*, vol. 716, pp. 30–61, 2012. DOI: 10.1016/j.physletb.2012.08.021. arXiv: 1207.7235 [hep-ex] (cit. on p. 7).

[23] C. Campagnari and M. Franklin, "The Discovery of the top quark," *Rev. Mod. Phys.*, vol. 69, pp. 137–212, 1997. DOI: 10.1103/RevModPhys.69.137. arXiv: hep-ex/9608003 (cit. on p. 7).

[24] P. M. Watkins, "DISCOVERY OF THE W AND Z BOSONS," *Contemp. Phys.*, vol. 27, pp. 291–324, 1986. DOI: 10.1080/00107518608211015 (cit. on p. 7).

[25] B. C. Odom, D. Hanneke, B. D'Urso and G. Gabrielse, "New Measurement of the Electron Magnetic Moment Using a One-Electron Quantum Cyclotron," *Phys. Rev. Lett.*, vol. 97, p. 030 801, 2006. DOI: 10.1103/PhysRevLett.97.030801 (cit. on p. 7).

[26] J. M. Maldacena, "Gravity, particle physics and their unification," *Int. J. Mod. Phys. A*, vol. 15S1, J. Jaros and M. E. Peskin, Eds., pp. 840–852, 2000. DOI: 10.1142/S0217751X00005449. arXiv: hep-ph/0002092 (cit. on p. 7).

[27] F. Marchesano, G. Shiu and T. Weigand, "The Standard Model from String Theory: What Have We Learned?," Jan. 2024. DOI: 10.1146/annurev-nucl-102622-01223. arXiv: 2401.01939 [hep-th] (cit. on p. 7).

[28] M. J. Mortonson, D. H. Weinberg and M. White, "Dark Energy: A Short Review," Dec. 2013. arXiv: 1401.0046 [astro-ph.CO] (cit. on p. 8).

[29] P. Binetruy, "Dark energy and fundamental physics," *J. Phys. Conf. Ser.*, vol. 171, J. Bernabeu, F. J. Botella, N. E. Mavromatos and V. A. Mitsou, Eds., p. 012 011, 2009. DOI: 10.1088/1742-6596/171/1/012011 (cit. on p. 8).

[30] L. Wang and P. J. Steinhardt, "Cluster abundance constraints for cosmological models with a time-varying, spatially inhomogeneous energy component with negative pressure," *The Astrophysical Journal*, vol. 508, no. 2, p. 483, 1998. DOI: 10.1086/306436. [Online]. Available: https://dx.doi.org/10.1086/306436 (cit. on p. 8).

[31] I. Zlatev, L. Wang and P. J. Steinhardt, "Quintessence, cosmic coincidence, and the cosmological constant," *Phys. Rev. Lett.*, vol. 82, pp. 896–899, 5 1999. DOI: 10.1103/PhysRevLett.82.896. [Online]. Available: https://link.aps.org/doi/10.1103/PhysRevLett.82.896 (cit. on p. 8).

[32] J. A. Frieman, C. T. Hill, A. Stebbins and I. Waga, "Cosmology with ultralight pseudo Nambu-Goldstone bosons," *Phys. Rev. Lett.*, vol. 75, pp. 2077–2080, 1995. DOI: 10.1103/PhysRevLett.75.2077. arXiv: astro-ph/9505060 (cit. on p. 8).

[33] B. Ratra and P. J. E. Peebles, "Cosmological Consequences of a Rolling Homogeneous Scalar Field," *Phys. Rev. D*, vol. 37, p. 3406, 1988. DOI: 10.1103/PhysRevD.37.3406 (cit. on p. 8).

[34] C. Wetterich, "Cosmology and the Fate of Dilatation Symmetry," *Nucl. Phys. B*, vol. 302, pp. 668–696, 1988. DOI: 10.1016/0550-3213(88)90193-9. arXiv: 1711.03844 [hep-th] (cit. on p. 8).

[35] E. Sather, "The Mystery of the matter asymmetry," *SLAC Beam Line*, vol. 26N1, pp. 31–37, 1996 (cit. on p. 8).

[36] L. Canetti, M. Drewes and M. Shaposhnikov, "Matter and Antimatter in the Universe," *New J. Phys.*, vol. 14, p. 095 012, 2012. DOI: 10.1088/1367-2630/14/9/095012. arXiv: 1204.4186 [hep-ph] (cit. on p. 8).

[37] Y. Fukuda *et al.*, "Evidence for oscillation of atmospheric neutrinos," *Phys. Rev. Lett.*, vol. 81, pp. 1562–1567, 1998. DOI: 10.1103/PhysRevLett.81.1562. arXiv: hep-ex/9807003 (cit. on p. 8).

[38] Q. R. Ahmad *et al.*, "Measurement of the rate of $\nu_e + d \to p + p + e^-$ interactions produced by ^{8}B solar neutrinos at the Sudbury Neutrino Observatory," *Phys. Rev. Lett.*, vol. 87, p. 071 301, 2001. DOI: 10.1103/PhysRevLett.87.071301. arXiv: nucl-ex/0106015 (cit. on p. 8).

[39] Q. R. Ahmad *et al.*, "Direct evidence for neutrino flavor transformation from neutral current interactions in the Sudbury Neutrino Observatory," *Phys. Rev. Lett.*, vol. 89, p. 011 301, 2002. DOI: 10.1103/PhysRevLett.89.011301. arXiv: nucl-ex/0204008 (cit. on p. 8).

[40] G. Bertone and D. Hooper, "History of dark matter," *Rev. Mod. Phys.*, vol. 90, no. 4, p. 045 002, 2018. DOI: 10.1103/RevModPhys.90.045002. arXiv: 1605.04909 [astro-ph.CO] (cit. on p. 8).

[41] "XII. Extract from the Translation of a Letter from Professor Bessel, dated Konigsberg, 10th of August, 1844. On the Variations of the Proper Motions of Procyon and Sirius," *Monthly Notices of the Royal Astronomical Society*, vol. 6, no. 11, pp. 136–141, Dec. 1844, ISSN: 0035-8711. DOI: 10.1093/mnras/6.11.136a. eprint: https://academic.oup.com/mnras/article-pdf/6/11/136/2872642/mnras6-0136a.pdf. [Online]. Available: https://doi.org/10.1093/mnras/6.11.136a (cit. on p. 8).

[42] W. Thomson Baron Kelvin, *Baltimore Lectures on Molecular Dynamics and the Wave Theory of Light* (Cambridge Library Collection - Physical Sciences). Cambridge University Press, 2010 (cit. on p. 8).

[43] H. Andernach and F. Zwicky, "English and Spanish Translation of Zwicky's (1933) The Redshift of Extragalactic Nebulae," Nov. 2017. arXiv: 1711.01693 [astro-ph.IM] (cit. on p. 8).

[44] D. Clowe, A. Gonzalez and M. Markevitch, "Weak lensing mass reconstruction of the interacting cluster 1E0657-558: Direct evidence for the existence of dark matter," *Astrophys. J.*, vol. 604, pp. 596–603, 2004. DOI: 10.1086/381970. arXiv: astro-ph/0312273 (cit. on p. 9).

[45] K. G. Begeman, A. H. Broeils and R. H. Sanders, "Extended rotation curves of spiral galaxies: Dark haloes and modified dynamics," *Mon. Not. Roy. Astron. Soc.*, vol. 249, p. 523, 1991. DOI: 10.1093/mnras/249.3.523 (cit. on p. 10).

[46] Y. Sofue and V. Rubin, "Rotation curves of spiral galaxies," *Ann. Rev. Astron. Astrophys.*, vol. 39, pp. 137–174, 2001. DOI: 10.1146/annurev.astro.39.1.137. arXiv: astro-ph/0010594 (cit. on p. 10).

[47] M. Kamionkowski and A. Kinkhabwala, "Galactic halo models and particle dark matter detection," *Phys. Rev. D*, vol. 57, pp. 3256–3263, 1998. DOI: 10.1103/PhysRevD.57.3256. arXiv: hep-ph/9710337 (cit. on p. 10).

[48] A. A. Dutton, A. V. Macciò, T. Buck, K. L. Dixon, M. Blank and A. Obreja, "NIHAO XX: the impact of the star formation threshold on the cusp–core transformation of cold dark matter haloes," *Mon. Not. Roy. Astron. Soc.*, vol. 486, no. 1, pp. 655–671, 2019. DOI: 10.1093/mnras/stz889. arXiv: 1811.10625 [astro-ph.GA] (cit. on p. 10).

[49] J. F. Navarro, C. S. Frenk and S. D. M. White, "The Structure of cold dark matter halos," *Astrophys. J.*, vol. 462, pp. 563–575, 1996. DOI: 10.1086/177173. arXiv: astro-ph/9508025 (cit. on p. 10).

[50] B. Moore, "Evidence against dissipationless dark matter from observations of galaxy haloes," *Nature*, vol. 370, p. 629, 1994. DOI: 10.1038/370629a0 (cit. on p. 10).

[51] H. Deng, M. P. Hertzberg, M. H. Namjoo and A. Masoumi, "Can Light Dark Matter Solve the Core-Cusp Problem?" *Phys. Rev. D*, vol. 98, no. 2, p. 023 513, 2018. DOI: 10.1103/PhysRevD.98.023513. arXiv: 1804.05921 [astro-ph.CO] (cit. on p. 10).

[52] C. S. Frenk and S. D. M. White, "Dark matter and cosmic structure," *Annalen Phys.*, vol. 524, pp. 507–534, 2012. DOI: 10.1002/andp.201200212. arXiv: 1210.0544 [astro-ph.CO] (cit. on p. 10).

[53] J. P. Ostriker and P. J. E. Peebles, "A Numerical Study of the Stability of Flattened Galaxies: or, can Cold Galaxies Survive?" *Astrophys. J.*, vol. 186, pp. 467–480, 1973. DOI: 10.1086/152513 (cit. on p. 10).

[54] S. D. M. White and M. J. Rees, "Core condensation in heavy halos: A Two stage theory for galaxy formation and clusters," *Mon. Not. Roy. Astron. Soc.*, vol. 183, pp. 341–358, 1978. DOI: 10.1093/mnras/183.3.341 (cit. on p. 11).

[55] W. Hu and S. Dodelson, "Cosmic Microwave Background Anisotropies," *Ann. Rev. Astron. Astrophys.*, vol. 40, pp. 171–216, 2002. DOI: 10.1146/annurev.astro.40.060401.093926. arXiv: astro-ph/0110414 (cit. on p. 11).

[56] P. Bull *et al.*, "Beyond ΛCDM: Problems, solutions, and the road ahead," *Phys. Dark Univ.*, vol. 12, pp. 56–99, 2016. DOI: 10.1016/j.dark.2016.02.001. arXiv: 1512.05356 [astro-ph.CO] (cit. on p. 11).

[57] D. J. Hegyi and K. A. Olive, "Can Galactic Halos Be Made of Baryons?" *Phys. Lett. B*, vol. 126, M. A. Srednicki, Ed., p. 28, 1983. DOI: 10.1016/0370-2693(83)90009-6 (cit. on p. 13).

[58] P. Tisserand *et al.*, "Limits on the Macho Content of the Galactic Halo from the EROS-2 Survey of the Magellanic Clouds," *Astron. Astrophys.*, vol. 469, pp. 387–404, 2007. DOI: 10.1051/0004-6361:20066017. arXiv: astro-ph/0607207 (cit. on p. 13).

[59] T. Lasserre and A. Milsztajn, "Not Enough Stellar Mass Machos In The Galactic Halo," in *35th Rencontres de Moriond: Cosmological Physics with Gravitational Lensing and 20th Moriond Astrophysics Meeting*, Les Ulis: EDP Sciences, 2001, pp. 21–24 (cit. on p. 13).

[60] P. Villanueva-Domingo, O. Mena and S. Palomares-Ruiz, "A brief review on primordial black holes as dark matter," *Front. Astron. Space Sci.*, vol. 8, p. 87, 2021. DOI: 10.3389/fspas.2021.681084. arXiv: 2103.12087 [astro-ph.CO] (cit. on p. 13).

[61] B. Carr and F. Kuhnel, "Primordial Black Holes as Dark Matter: Recent Developments," *Ann. Rev. Nucl. Part. Sci.*, vol. 70, pp. 355–394, 2020. DOI: 10.1146/annurev-nucl-050520-125911. arXiv: 2006.02838 [astro-ph.CO] (cit. on p. 13).

[62] M. Milgrom, "A Modification of the Newtonian dynamics: Implications for galaxies," *Astrophys. J.*, vol. 270, pp. 371–383, 1983. DOI: 10.1086/161131 (cit. on p. 13).

[63] M. Milgrom, "A modification of the Newtonian dynamics: implications for galaxy systems," *Astrophys. J.*, vol. 270, pp. 384–389, 1983. DOI: 10.1086/161132 (cit. on p. 13).

[64] A. Aguirre, J. Schaye and E. Quataert, "Problems for MOND in clusters and the Ly-alpha forest," *Astrophys. J.*, vol. 561, p. 550, 2001. DOI: 10.1086/323376. arXiv: astro-ph/0105184 (cit. on p. 13).

[65] D. Clowe, M. Bradac, A. H. Gonzalez *et al.*, "A direct empirical proof of the existence of dark matter," *Astrophys. J. Lett.*, vol. 648, pp. L109–L113, 2006. DOI: 10.1086/508162. arXiv: astro-ph/0608407 (cit. on p. 13).

[66] P. J. E. Peebles, "PRIMEVAL ADIABATIC PERTURBATIONS: EFFECT OF MASSIVE NEUTRINOS," *Astrophys. J.*, vol. 258, pp. 415–424, 1982. DOI: 10.1086/160094 (cit. on p. 13).

[67] S. D. M. White, C. S. Frenk and M. Davis, "Clustering in a Neutrino Dominated Universe," *Astrophys. J. Lett.*, vol. 274, M. A. Srednicki, Ed., pp. L1–L5, 1983. DOI: 10.1086/161425 (cit. on p. 13).

[68] S. Tremaine and J. E. Gunn, "Dynamical Role of Light Neutral Leptons in Cosmology," *Phys. Rev. Lett.*, vol. 42, M. A. Srednicki, Ed., pp. 407–410, 1979. DOI: 10.1103/PhysRevLett.42.407 (cit. on pp. 13, 19).

[69] G. Steigman and M. S. Turner, "Cosmological Constraints on the Properties of Weakly Interacting Massive Particles," *Nucl. Phys. B*, vol. 253, pp. 375–386, 1985. DOI: 10.1016/0550-3213(85)90537-1 (cit. on p. 14).

[70] K. Saikawa and S. Shirai, "Precise WIMP Dark Matter Abundance and Standard Model Thermodynamics," *JCAP*, vol. 08, p. 011, 2020. DOI: 10.1088/1475-7516/2020/08/011. arXiv: 2005.03544 [hep-ph] (cit. on p. 14).

[71] M. Schumann, "Direct Detection of WIMP Dark Matter: Concepts and Status," *J. Phys. G*, vol. 46, no. 10, p. 103 003, 2019. DOI: 10.1088/1361-6471/ab2ea5. arXiv: 1903.03026 [astro-ph.CO] (cit. on pp. 14, 18).

[72] F. S. Queiroz, "WIMP Theory Review," *PoS*, vol. EPS-HEP2017, P. Checchia *et al.*, Eds., p. 080, 2017. DOI: 10.22323/1.314.0080. arXiv: 1711.02463 [hep-ph] (cit. on p. 14).

[73] G. Arcadi, M. Dutra, P. Ghosh *et al.*, "The waning of the WIMP? A review of models, searches, and constraints," *Eur. Phys. J. C*, vol. 78, no. 3, p. 203, 2018. DOI: 10.1140/epjc/s10052-018-5662-y. arXiv: 1703.07364 [hep-ph] (cit. on p. 14).

[74] B. W. Lee and S. Weinberg, "Cosmological Lower Bound on Heavy Neutrino Masses," *Phys. Rev. Lett.*, vol. 39, M. A. Srednicki, Ed., pp. 165–168, 1977. DOI: 10.1103/PhysRevLett.39.165 (cit. on p. 14).

[75] P. Gondolo and G. Gelmini, "Cosmic abundances of stable particles: Improved analysis," *Nucl. Phys. B*, vol. 360, pp. 145–179, 1991. DOI: 10.1016/0550-3213(91)90438-4 (cit. on pp. 14, 15, 17).

[76] M. Srednicki, R. Watkins and K. A. Olive, "Calculations of Relic Densities in the Early Universe," *Nucl. Phys. B*, vol. 310, M. A. Srednicki, Ed., p. 693, 1988. DOI: 10.1016/0550-3213(88)90099-5 (cit. on p. 14).

[77] C. Cosme, M. Dutra, S. Godfrey and T. R. Gray, "Testing freeze-in with axial and vector Z' bosons," *JHEP*, vol. 09, p. 056, 2021. DOI: 10.1007/JHEP09(2021)056. arXiv: 2104.13937 [hep-ph] (cit. on p. 14).

[78] E. W. Kolb and M. S. Turner, *The Early Universe*. 1990, vol. 69, ISBN: 978-0-201-62674-2. DOI: 10.1201/9780429492860 (cit. on p. 15).

[79] T. R. Gray, "How was Dark Matter Produced in the Early Universe? A Study of Fermionic Dark Matter with a Z-prime Portal," M.S. thesis, Ottawa U., 2020 (cit. on pp. 15, 17).

[80] L. Husdal, "On Effective Degrees of Freedom in the Early Universe," *Galaxies*, vol. 4, no. 4, p. 78, 2016. DOI: 10.3390/galaxies4040078. arXiv: 1609.04979 [astro-ph.CO] (cit. on p. 16).

[81] J. de Dios Zornoza, "Review on Indirect Dark Matter Searches with Neutrino Telescopes," *Universe*, vol. 7, no. 11, p. 415, 2021. DOI: 10.3390/universe7110415 (cit. on p. 18).

[82] C. Pérez de los Heros, "Status, Challenges and Directions in Indirect Dark Matter Searches," *Symmetry*, vol. 12, no. 10, p. 1648, 2020. DOI: 10.3390/sym12101648. arXiv: 2008.11561 [astro-ph.HE] (cit. on p. 18).

[83] T. R. Slatyer, "Indirect dark matter signatures in the cosmic dark ages. I. Generalizing the bound on s-wave dark matter annihilation from Planck results," *Phys. Rev. D*, vol. 93, no. 2, p. 023 527, 2016. DOI: 10.1103/PhysRevD.93.023527. arXiv: 1506.03811 [hep-ph] (cit. on p. 18).

[84] T. R. Slatyer, "Indirect Dark Matter Signatures in the Cosmic Dark Ages II. Ionization, Heating and Photon Production from Arbitrary Energy Injections," *Phys. Rev. D*, vol. 93, no. 2, p. 023 521, 2016. DOI: 10.1103/PhysRevD.93.023521. arXiv: 1506.03812 [astro-ph.CO] (cit. on p. 18).

[85] R. Catena, D. Cole, T. Emken *et al.*, "Dark matter-electron interactions in materials beyond the dark photon model," *JCAP*, vol. 03, p. 052, 2023. DOI: 10.1088/1475-7516/2023/03/052. arXiv: 2210.07305 [hep-ph] (cit. on pp. 18, 21, 27).

[86] D. S. Akerib *et al.*, "Snowmass2021 Cosmic Frontier Dark Matter Direct Detection to the Neutrino Fog," in *Snowmass 2021*, Mar. 2022. arXiv: 2203.08084 [hep-ex] (cit. on p. 18).

[87] M. Graham, C. Hearty and M. Williams, "Searches for Dark Photons at Accelerators," *Ann. Rev. Nucl. Part. Sci.*, vol. 71, pp. 37–58, 2021. DOI: 10.1146/annurev-nucl-110320-051823. arXiv: 2104.10280 [hep-ph] (cit. on p. 18).

[88] D. Perez Adan, "Dark Matter searches at CMS and ATLAS," in *56th Rencontres de Moriond on Electroweak Interactions and Unified Theories*, Jan. 2023. arXiv: 2301.10141 [hep-ex] (cit. on p. 18).

[89] J. P. Lees *et al.*, "Search for Invisible Decays of a Dark Photon Produced in e^+e^- Collisions at BaBar," *Phys. Rev. Lett.*, vol. 119, no. 13, p. 131 804, 2017. DOI: 10.1103/PhysRevLett.119.131804. arXiv: 1702.03327 [hep-ex] (cit. on pp. 19, 26).

[90] W. Altmannshofer *et al.*, "The Belle II Physics Book," *PTEP*, vol. 2019, no. 12, E. Kou and P. Urquijo, Eds., p. 123C01, 2019, [Erratum: PTEP 2020, 029201 (2020)]. DOI: 10.1093/ptep/ptz106. arXiv: 1808.10567 [hep-ex] (cit. on pp. 19, 26).

[91] X. Chu, J.-L. Kuo and J. Pradler, "Toward a full description of MeV dark matter decoupling: A self-consistent determination of relic abundance and Neff," *Phys. Rev. D*, vol. 106, no. 5, p. 055 022, 2022. DOI: 10.1103/PhysRevD.106.055022. arXiv: 2205.05714 [hep-ph] (cit. on p. 19).

[92] M. Battaglieri *et al.*, "US Cosmic Visions: New Ideas in Dark Matter 2017: Community Report," in *U.S. Cosmic Visions: New Ideas in Dark Matter*, Jul. 2017. arXiv: 1707.04591 [hep-ph] (cit. on pp. 19, 21, 22).

[93] M. Fabbrichesi, E. Gabrielli and G. Lanfranchi, "The Dark Photon," May 2020. DOI: 10.1007/978-3-030-62519-1. arXiv: 2005.01515 [hep-ph] (cit. on pp. 20, 26).

[94] B. Holdom, "Two U(1)'s and Epsilon Charge Shifts," *Phys. Lett. B*, vol. 166, pp. 196–198, 1986. DOI: 10.1016/0370-2693(86)91377-8 (cit. on p. 20).

[95] K. S. Babu, C. F. Kolda and J. March-Russell, "Implications of generalized Z - Z-prime mixing," *Phys. Rev. D*, vol. 57, pp. 6788–6792, 1998. DOI: 10.1103/PhysRevD.57.6788. arXiv: hep-ph/9710441 (cit. on p. 20).

[96] E. C. G. Stueckelberg, "Interaction energy in electrodynamics and in the field theory of nuclear forces," *Helv. Phys. Acta*, vol. 11, pp. 225–244, 1938. DOI: 10.5169/seals-110852 (cit. on p. 20).

[97] R. Catena and T. R. Gray, "Spin-1 thermal targets for dark matter searches at beam dump and fixed target experiments," *JCAP*, vol. 11, p. 058, 2023. DOI: 10.1088/1475-7516/2023/11/058. arXiv: 2307.02207 [hep-ph] (cit. on pp. 20, 27, 29).

[98] S. Balan *et al.*, "Resonant or asymmetric: The status of sub-GeV dark matter," May 2024. arXiv: 2405.17548 [hep-ph] (cit. on pp. 20, 33, 36, 38).

[99] R. Essig, J. Mardon and T. Volansky, "Direct Detection of Sub-GeV Dark Matter," *Phys. Rev. D*, vol. 85, p. 076 007, 2012. DOI: 10.1103/PhysRevD.85.076007. arXiv: 1108.5383 [hep-ph] (cit. on p. 21).

[100] A. Berlin, P. deNiverville, A. Ritz, P. Schuster and N. Toro, "Sub-GeV dark matter production at fixed-target experiments," *Phys. Rev. D*, vol. 102, no. 9, p. 095 011, 2020. DOI: 10.1103/PhysRevD.102.095011. arXiv: 2003.03379 [hep-ph] (cit. on p. 21).

[101] J. D. Bjorken, R. Essig, P. Schuster and N. Toro, "New Fixed-Target Experiments to Search for Dark Gauge Forces," *Phys. Rev. D*, vol. 80, p. 075 018, 2009. DOI: 10.1103/PhysRevD.80.075018. arXiv: 0906.0580 [hep-ph] (cit. on p. 21).

[102] P. deNiverville, C.-Y. Chen, M. Pospelov and A. Ritz, "Light dark matter in neutrino beams: production modelling and scattering signatures at MiniBooNE, T2K and SHiP," *Phys. Rev. D*, vol. 95, no. 3, p. 035 006, 2017. DOI: 10.1103/PhysRevD.95.035006. arXiv: 1609.01770 [hep-ph] (cit. on pp. 21, 23, 24).

[103] B. Batell, M. Pospelov and A. Ritz, "Exploring Portals to a Hidden Sector Through Fixed Targets," *Phys. Rev. D*, vol. 80, p. 095 024, 2009. DOI: 10.1103/PhysRevD.80.095024. arXiv: 0906.5614 [hep-ph] (cit. on p. 21).

[104] A. Berlin, N. Blinov, G. Krnjaic, P. Schuster and N. Toro, "Dark Matter, Millicharges, Axion and Scalar Particles, Gauge Bosons, and Other New Physics with LDMX," *Phys. Rev. D*, vol. 99, no. 7, p. 075 001, 2019. DOI: 10.1103/PhysRevD.99.075001. arXiv: 1807.01730 [hep-ph] (cit. on pp. 21, 23).

[105] A. A. Aguilar-Arevalo *et al.*, "Dark Matter Search in a Proton Beam Dump with MiniBooNE," *Phys. Rev. Lett.*, vol. 118, no. 22, p. 221 803, 2017. DOI: 10.1103/PhysRevLett.118.221803. arXiv: 1702.02688 [hep-ex] (cit. on p. 21).

[106] A. A. Aguilar-Arevalo *et al.*, "Dark Matter Search in Nucleon, Pion, and Electron Channels from a Proton Beam Dump with MiniBooNE," *Phys. Rev. D*, vol. 98, no. 11, p. 112 004, 2018. DOI: 10.1103/PhysRevD.98.112004. arXiv: 1807.06137 [hep-ex] (cit. on p. 21).

[107] L. B. Auerbach *et al.*, "Measurement of electron - neutrino - electron elastic scattering," *Phys. Rev. D*, vol. 63, p. 112 001, 2001. DOI: 10.1103/PhysRevD.63.112001. arXiv: hep-ex/0101039 (cit. on p. 22).

[108] P. deNiverville, M. Pospelov and A. Ritz, "Observing a light dark matter beam with neutrino experiments," *Phys. Rev. D*, vol. 84, p. 075 020, 2011. DOI: 10.1103/PhysRevD.84.075020. arXiv: 1107.4580 [hep-ph] (cit. on p. 22).

[109] C Athanassopoulos *et al.*, "The Liquid scintillator neutrino detector and LAMPF neutrino source," *Nucl. Instrum. Meth. A*, vol. 388, pp. 149–172, 1997. DOI: 10.1016/S0168-9002(96)01155-2. arXiv: nucl-ex/9605002 (cit. on p. 22).

[110] Y. M. Andreev *et al.*, "Search for Light Dark Matter with NA64 at CERN," *Phys. Rev. Lett.*, vol. 131, no. 16, p. 161 801, 2023. DOI: 10.1103/PhysRevLett.131.161801. arXiv: 2307.02404 [hep-ex] (cit. on p. 22).

[111] T. Åkesson *et al.*, "Current Status and Future Prospects for the Light Dark Matter eXperiment," in *Snowmass 2021*, Mar. 2022. arXiv: 2203.08192 [hep-ex] (cit. on p. 23).

[112] T. Åkesson *et al.*, "Light Dark Matter eXperiment (LDMX)," Aug. 2018. arXiv: 1808.05219 [hep-ex] (cit. on pp. 23, 25, 26).

[113] Y. Kahn, G. Krnjaic, J. Thaler and M. Toups, "DAEδALUS and dark matter detection," *Phys. Rev. D*, vol. 91, no. 5, p. 055 006, 2015. DOI: 10.1103/PhysRevD.91.055006. arXiv: 1411.1055 [hep-ph] (cit. on pp. 23, 24).

[114] Y.-S. Liu and G. A. Miller, "Validity of weizsäcker-williams approximation and the analysis of beam dump experiments: Production of an axion, a dark photon, or a new axial-vector boson," *Physical Review D*, vol. 96, no. 1, 2017, ISSN: 2470-0029. DOI: 10.1103/physrevd.96.016004. [Online]. Available: http://dx.doi.org/10.1103/PhysRevD.96.016004 (cit. on p. 24).

[115] K. J. Kim and Y.-S. Tsai, "IMPROVED WEIZSACKER-WILLIAMS METHOD AND ITS APPLICATION TO LEPTON AND W BOSON PAIR PRODUCTION," *Phys. Rev. D*, vol. 8, p. 3109, 1973. DOI: 10.1103/PhysRevD.8.3109 (cit. on p. 24).

[116] J. Blümlein and J. Brunner, "New Exclusion Limits on Dark Gauge Forces from Proton Bremsstrahlung in Beam-Dump Data," *Phys. Lett. B*, vol. 731, pp. 320–326, 2014. DOI: 10.1016/j.physletb.2014.02.029. arXiv: 1311.3870 [hep-ph] (cit. on p. 24).

[117] J. Alwall, M. Herquet, F. Maltoni, O. Mattelaer and T. Stelzer, "MadGraph 5 : Going Beyond," *JHEP*, vol. 06, p. 128, 2011. DOI: 10.1007/JHEP06(2011)128. arXiv: 1106.0522 [hep-ph] (cit. on p. 25).

[118] C. Degrande, C. Duhr, B. Fuks, D. Grellscheid, O. Mattelaer and T. Reiter, "UFO - The Universal FeynRules Output," *Comput. Phys. Commun.*, vol. 183, pp. 1201–1214, 2012. DOI: 10.1016/j.cpc.2012.01.022. arXiv: 1108.2040 [hep-ph] (cit. on p. 25).

[119] J. D. Bjorken, R. Essig, P. Schuster and N. Toro, "New fixed-target experiments to search for dark gauge forces," *Physical Review D*, vol. 80, no. 7, 2009, ISSN: 1550-2368. DOI: 10.1103/physrevd.80.075018. [Online]. Available: http://dx.doi.org/10.1103/PhysRevD.80.075018 (cit. on p. 25).

[120] J. B. Dent, L. M. Krauss, J. L. Newstead and S. Sabharwal, "General analysis of direct dark matter detection: From microphysics to observational signatures," *Phys. Rev. D*, vol. 92, no. 6, p. 063 515, 2015. DOI: 10.1103/PhysRevD.92.063515. arXiv: 1505.03117 [hep-ph] (cit. on p. 27).

[121] D. Alves, "Simplified Models for LHC New Physics Searches," *J. Phys. G*, vol. 39, N. Arkani-Hamed *et al.*, Eds., p. 105 005, 2012. DOI: 10.1088/0954-3899/39/10/105005. arXiv: 1105.2838 [hep-ph] (cit. on p. 27).

[122] R. Catena, J. Conrad and M. B. Krauss, "Compatibility of a dark matter discovery at XENONnT or LZ with the WIMP thermal production mechanism," *Phys. Rev. D*, vol. 97, no. 10, p. 103 002, 2018. DOI: 10.1103/PhysRevD.97.103002. arXiv: 1712.07969 [hep-ph] (cit. on p. 28).

[123] M. S. Chanowitz, M. A. Furman and I. Hinchliffe, "Weak Interactions of Ultraheavy Fermions. 2.," *Nucl. Phys. B*, vol. 153, pp. 402–430, 1979. DOI: 10.1016/0550-3213(79)90606-0 (cit. on p. 28).

[124] A. Schuessler and D. Zeppenfeld, "Unitarity constraints on MSSM trilinear couplings," in *15th International Conference on Supersymmetry and the Unification of Fundamental Interactions (SUSY07)*, Oct. 2007, pp. 236–239. arXiv: 0710.5175 [hep-ph] (cit. on p. 28).

[125] F. Kahlhoefer, K. Schmidt-Hoberg, T. Schwetz and S. Vogl, "Implications of unitarity and gauge invariance for simplified dark matter models," *JHEP*, vol. 02, p. 016, 2016. DOI: 10.1007/JHEP02(2016)016. arXiv: 1510.02110 [hep-ph] (cit. on p. 28).

[126] C. Chang, P. Scott, T. E. Gonzalo, F. Kahlhoefer and M. White, "Global fits of simplified models for dark matter with GAMBIT: II. Vector dark matter with an s-channel vector mediator," *Eur. Phys. J. C*, vol. 83, no. 8, p. 692, 2023, [Erratum: Eur.Phys.J.C 83, 768 (2023)]. DOI: 10.1140/epjc/s10052-023-11859-3. arXiv: 2303.08351 [hep-ph] (cit. on p. 29).

[127] S.-M. Choi, H. M. Lee, Y. Mambrini and M. Pierre, "Vector SIMP dark matter with approximate custodial symmetry," *JHEP*, vol. 07, p. 049, 2019. DOI: 10.1007/JHEP07(2019)049. arXiv: 1904.04109 [hep-ph] (cit. on pp. 29, 30).

[128] Y. Hochberg, E. Kuflik, T. Volansky and J. G. Wacker, "Mechanism for Thermal Relic Dark Matter of Strongly Interacting Massive Particles," *Phys. Rev. Lett.*, vol. 113, p. 171 301, 2014. DOI: 10.1103/PhysRevLett.113.171301. arXiv: 1402.5143 [hep-ph] (cit. on p. 29).

[129] S.-M. Choi, Y. Hochberg, E. Kuflik *et al.*, "Vector SIMP dark matter," *JHEP*, vol. 10, p. 162, 2017. DOI: 10.1007/JHEP10(2017)162. arXiv: 1707.01434 [hep-ph] (cit. on p. 29).

[130] S. S. AbdusSalam *et al.*, "Simple and statistically sound recommendations for analysing physical theories," *Rept. Prog. Phys.*, vol. 85, no. 5, p. 052 201, 2022. DOI: 10.1088/1361-6633/ac60ac. arXiv: 2012.09874 [hep-ph] (cit. on p. 33).

[131] P. Athron *et al.*, "GAMBIT: The Global and Modular Beyond-the-Standard-Model Inference Tool," *Eur. Phys. J. C*, vol. 77, no. 11, p. 784, 2017, [Addendum: Eur.Phys.J.C 78, 98 (2018)]. DOI: 10.1140/epjc/s10052-017-5321-8. arXiv: 1705.07908 [hep-ph] (cit. on p. 34).

[132] C. Balázs *et al.*, "ColliderBit: a GAMBIT module for the calculation of high-energy collider observables and likelihoods," *Eur. Phys. J. C*, vol. 77, no. 11, p. 795, 2017. DOI: 10.1140/epjc/s10052-017-5285-8. arXiv: 1705.07919 [hep-ph] (cit. on p. 34).

[133] M. Cirelli, N. Fornengo, J. Koechler, E. Pinetti and B. M. Roach, "Putting all the X in one basket: Updated X-ray constraints on sub-GeV Dark Matter," *JCAP*, vol. 07, p. 026, 2023. DOI: 10.1088/1475-7516/2023/07/026. arXiv: 2303.08854 [hep-ph] (cit. on p. 35).